The Phase Field Crystal Method: Strengths and Weaknesses

A. Yamanaka[1] , E. Alster, K.S. McReynolds, and P.W. Voorhees

Department of Materials Science and Engineering
Engineering Sciences and Applied Mathematics
Northwestern University

[1]Division of Advanced Mechanical Systems Engineering
Institute of Engineering
Tokyo University of Agriculture and Technology

Outline

- Introduction to the phase field crystal model
- Creating crystal structures
- Grain growth in 3D
- Future outlook, remaining challenges

Atomistic Simulation Methods

MD simulations

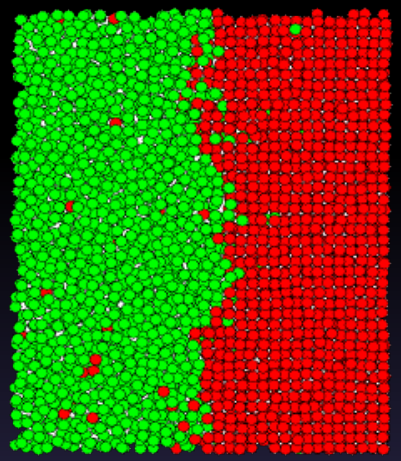

- Lattice vibration (ps)
- Fundamental physics

Cu-Au, M. Asta, J.J Hoyt

PFC Model
Elder et al.
(Swift-Hohenberg type free energy)

- Mean field theory:
  ϕ : Time averaged density
- Atomistic length scale
- Diffusive time scale (μs-ms)
- Multiple crystalline planes
- Elasticity
- Dislocations

Traditional Phase Field Theories

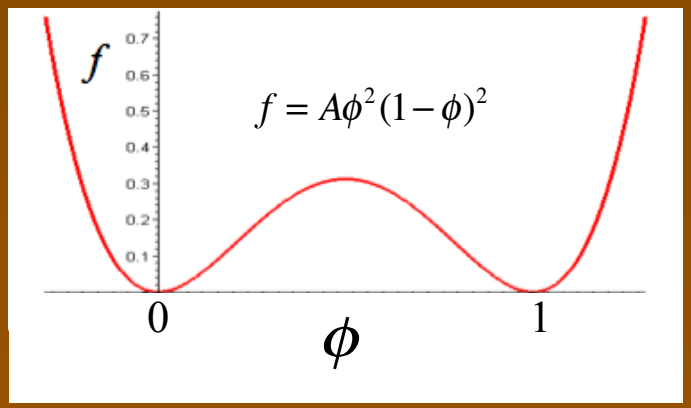

Minimize F:

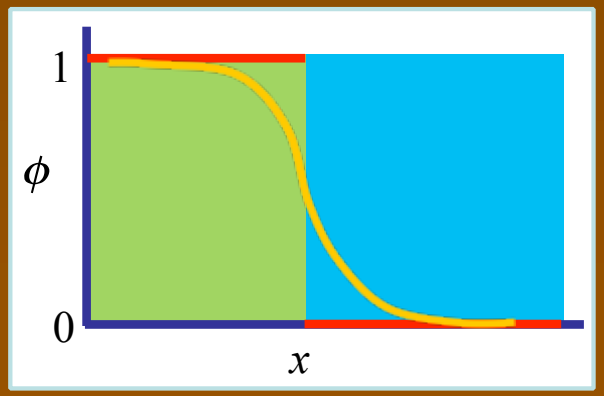

$$F(\phi) = \int \left[f(\phi) + K\left(\frac{\partial \phi}{\partial x}\right)^2 \right] dx$$

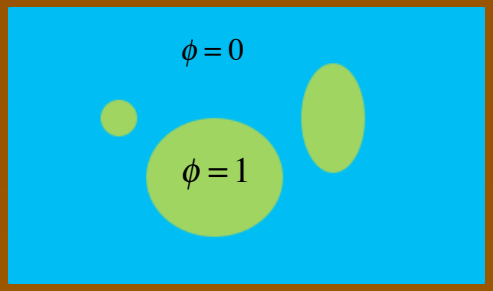

Two-phase mixture

Periodic Systems

$$F(\phi)=\int\left[f(\phi)+K\left(\frac{\partial\phi}{\partial x}\right)^2\right]dx$$

$$F(\phi)=\int\left[f(\phi)-K\left(\frac{\partial\phi}{\partial x}\right)^2\right]dx$$

$$F(\phi)=\int\left[f(\phi)-K\left(\frac{\partial\phi}{\partial x}\right)^2+\frac{1}{2}\left(\frac{\partial^2\phi}{\partial x^2}\right)\right]dx$$

$$F(\phi)=\int\left[f(\phi)-K\left(\frac{\partial\phi}{\partial x}\right)^2+\frac{1}{2}\left(\frac{\partial^2\phi}{\partial x^2}\right)^2\right]dx$$

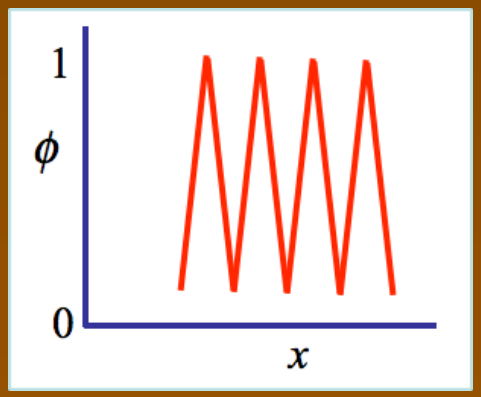

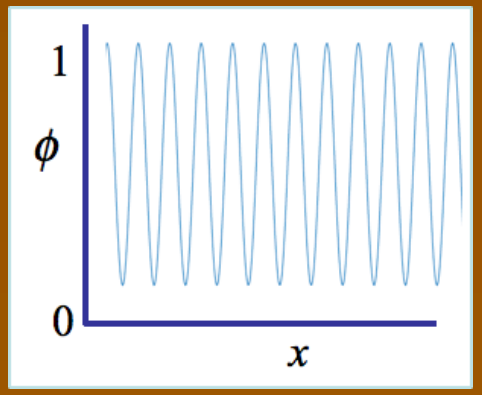

Periodic Systems

$$F(\phi) = \int \left[f(\phi) - q_o^2 \left(\frac{\partial \phi}{\partial x} \right)^2 + \frac{1}{2} \left(\frac{\partial^2 \phi}{\partial x^2} \right)^2 \right] dx$$

$$f(\phi) = \frac{1}{2}(-\epsilon + q_o^4)\phi^2 + \frac{1}{4}\phi^4$$

$$F(\phi) = \int \left[\frac{\phi}{2} \left(-\epsilon + \left(q_o^2 + \nabla^2 \right)^2 \right) \phi + \frac{1}{4}\phi^4 \right] dx$$

Swift-Hohenberg equation

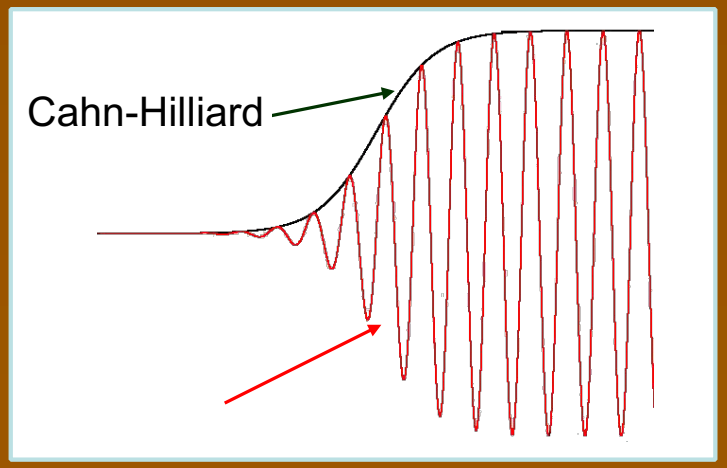

PFC 2D Phase Diagram

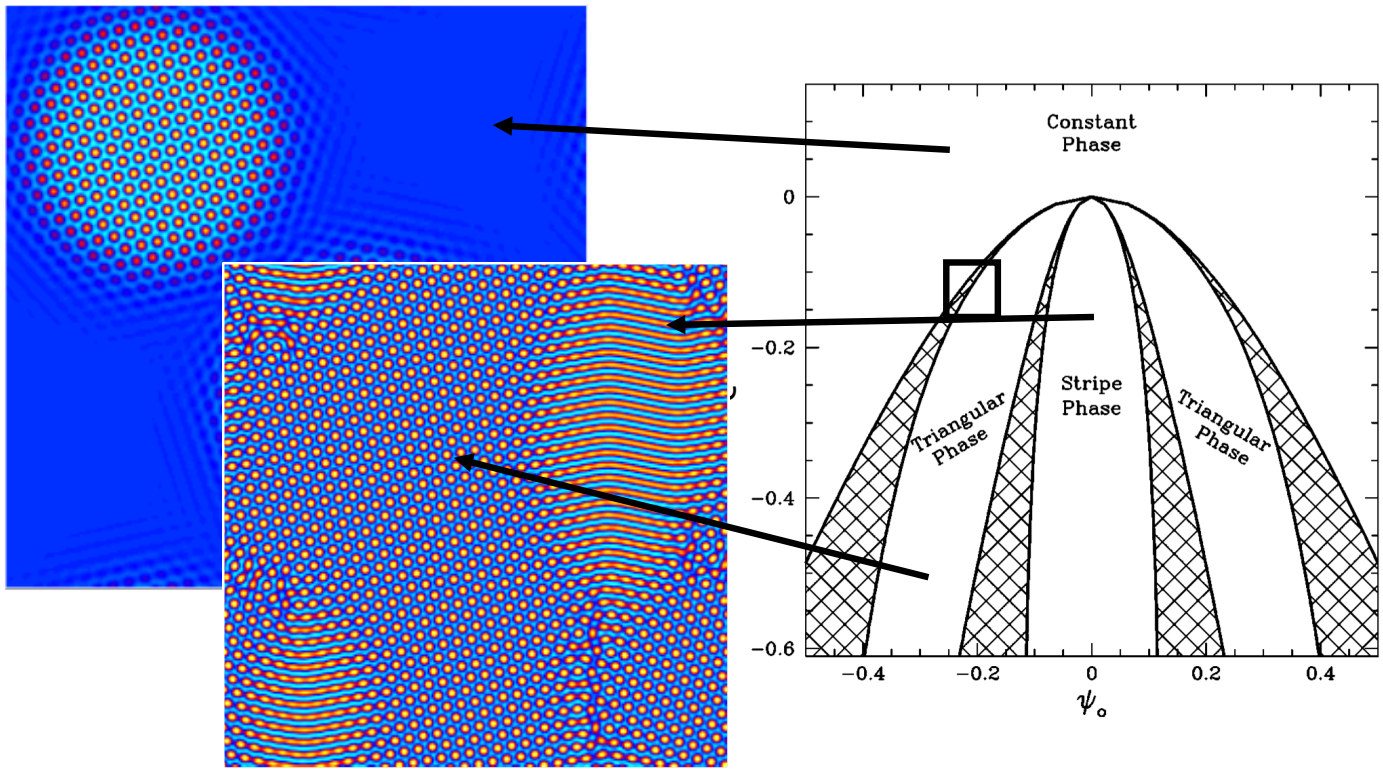

K.R. Elder and M. Grant, *Phys. Rev. E* **70**, 051605 (2004)

From Ramakrishnan and Youssoff, expanding around a liquid of uniform density relative to an ideal gas:

$$\frac{F}{k_B T \rho_o} = \int \left[(1 + n(\mathbf{r})) \ln (1 + n(\mathbf{r})) - n(\mathbf{r}) \right] d\mathbf{r} - \frac{1}{2} \int n(\mathbf{r}) C \left(|\mathbf{r} - \mathbf{r}'| \right) n(\mathbf{r}') d\mathbf{r} d\mathbf{r}'$$

$$n(\mathbf{r}) = \left(\rho(\mathbf{r}) - \rho_o \right) / \rho_o$$

Advantage: density field evolves on diffusional time scales

Disadvantage: Minimize F, in the crystal:

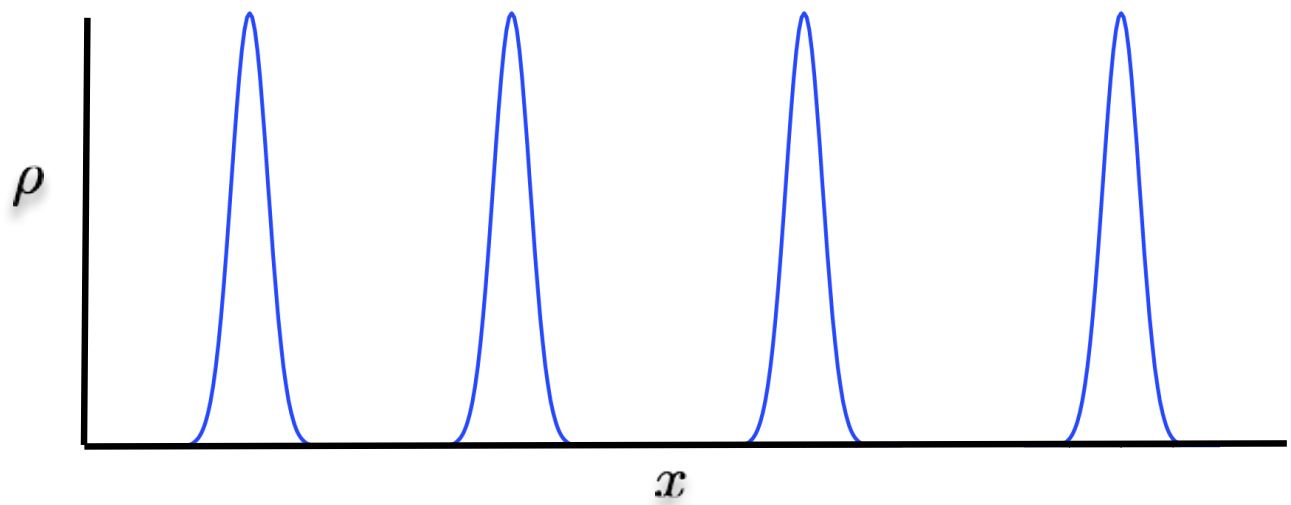

Expand about the mean density of the liquid:

$$\int \left[(1+n(\mathbf{r}))\ln(1+n(\mathbf{r})) - n(\mathbf{r})\right] d\mathbf{r} \sim \int \left[\frac{1}{2}n(\mathbf{r})^2 - a_1\frac{1}{6}n(\mathbf{r})^3 + a_2\frac{1}{12}n(\mathbf{r})^4\right] d\mathbf{r}$$

Require liquid to be present to lowest order in n: $a_1 = 0, a_2 = 3$

Expand the two-point correlation function,

$$-\frac{1}{2}\int n(\mathbf{r})C\left(|\mathbf{r}-\mathbf{r}'|\right)n(\mathbf{r}')d\mathbf{r}d\mathbf{r}'$$

$$C''(K_o) = S''(K_o)/S(K_o)^2$$

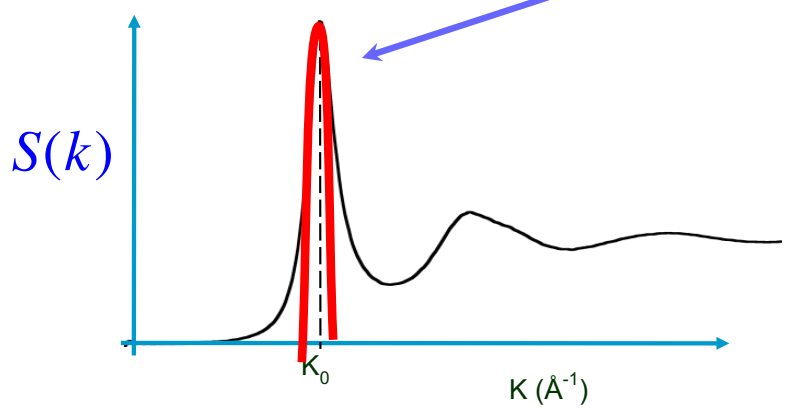

Elder, Provatas, Berry, Stefanovic, Grant, PRE 2007

$$F = \int \left\{ \frac{n(\mathbf{r})}{2}\left[-\epsilon + \left(\nabla^2+1\right)^2\right] n(\mathbf{r}) + \frac{1}{4}n^4(\mathbf{r}) \right\} d\mathbf{r}$$

$$\epsilon = \frac{8}{(1-3\psi_c^2)K_o^2 S(K_o)C''(K_o)}$$

Phase Field Crystal Approximation

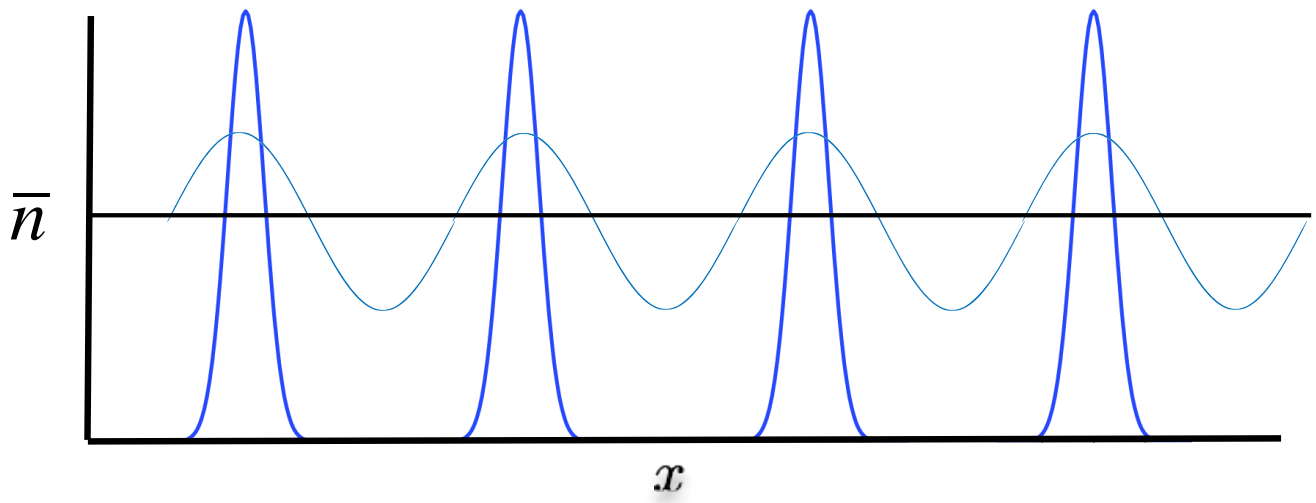

PFC parameter fitting

, **Fitting to Iron, T = 1772 K**

Quantity	Experiment/ MD	5 parameter [1]	6 parameter [2]
surface energy (100) (ergs/cm^2)	177.0 [1]	207.1	165.7
surface energy (110) (ergs/cm^2)	173.5 [1]	201.7	161.5
surface energy (111) (ergs/cm^2)	173.4 [1]	194.8	157.2
Anisotropy (%)	1.0 [1]	1.3	1.3
Expansion upon melting (Å^3/atom)	0.38 [3]	2.07	0.43
Solid bulk modulus (GPa)	105.0 [4]	22.2	94.5
Liquid bulk modulus (GPa)	96.2 [5]	18.6	93.2

[1] Wu, Karma, PRB, **76**, 174107 (2007)
[2] Jaatinen, Achim, Elder, Ala-Nissilä, PRB **80**, 031602 (2009).
[3] Mendelev, Han, Srolovitz, Ackland, Sun, Asta, Phil. Mag. **83**, 3977 (2003)
[4] Dever, J. Appl. Phys., **43**, 3293 (1972):
Adams, Agosta, Leisure, Ledbetter, J. Appl. Phys. **100**, 113530 (2006)
[5] Tsu, Takano, 88th Spring Conference (Japan Institute of Metals, Sendai 1981), **88**, p. 86:
Itami, Shimoji, J. Phys. F: Met. Phys, **14**, L15 (1984).

(due to Ken Elder)

PFC parameter fitting

Fitting to Iron, T = 1772 K

Quantity	Experiment/ MD	5 parameter [1]	6 parameter [2]
surface energy (100) (ergs/cm^2)	177.0 [1]	207.1 17%	165.7 6%
surface energy (110) (ergs/cm^2)	173.5 [1]	201.7 16%	161.5 7%
surface energy (111) (ergs/cm^2)	173.4 [1]	194.8 12%	157.2 9%
Anisotropy (%)	1.0 [1]	1.3 30%	1.3 30%
Expansion upon melting (Å^3/atom)	0.38 [3]	2.07	0.43
Solid bulk modulus (GPa)	105.0 [4]	22.2	94.5
Liquid bulk modulus (GPa)	96.2 [5]	18.6	93.2

percent error

[1] Wu, Karma, PRB, **76**, 174107 (2007)
[2] Jaatinen, Achim, Elder, Ala-Nissilä, PRB **80**, 031602 (2009).
[3] Mendelev, Han, Srolovitz, Ackland, Sun, Asta, Phil. Mag. **83**, 3977 (2003)
[4] Dever, J. Appl. Phys., **43**, 3293 (1972):
Adams, Agosta, Leisure, Ledbetter, J. Appl. Phys. **100**, 113530 (2006)
[5] Tsu, Takano, 88th Spring Conference (Japan Institute of Metals, Sendai 1981), **88**, p. 86:
Itami, Shimoji, J. Phys. F: Met. Phys, **14**, L15 (1984).

(due to Ken Elder)

* PFC parameter fitting

Fitting to Iron, T = 1772 K

Quantity	Experiment/ MD	5 parameter [1]	6 parameter [2]
surface energy (100) (ergs/cm^2)	177.0 [1]	207.1	165.7
surface energy (110) (ergs/cm^2)	173.5 [1]	201.7	161.5
surface energy (111) (ergs/cm^2)	173.4 [1]	194.8	157.2
Anisotropy (%)	1.0 [1]	1.3	1.3
Expansion upon melting (Å^3/atom)	0.38 [3]	2.07 440%	0.43 13%
Solid bulk modulus (GPa)	105.0 [4]	22.2 79%	94.5 10%
Liquid bulk modulus (GPa)	96.2 [5]	18.6 81%	93.2 3%

percent error

[1] Wu, Karma, PRB, **76**, 174107 (2007)
[2] Jaatinen, Achim, Elder, Ala-Nissilä, PRB **80**, 031602 (2009).
[3] Mendelev, Han, Srolovitz, Ackland, Sun, Asta, Phil. Mag. **83**, 3977 (2003)
[4] Dever, J. Appl. Phys., **43**, 3293 (1972):
Adams, Agosta, Leisure, Ledbetter, J. Appl. Phys. **100**, 113530 (2006)
[5] Tsu, Takano, 88th Spring Conference (Japan Institute of Metals, Sendai 1981), **88**, p. 86:
Itami, Shimoji, J. Phys. F: Met. Phys, **14**, L15 (1984).

(due to Ken Elder)

Solid-Liquid Interfacial Density Profile

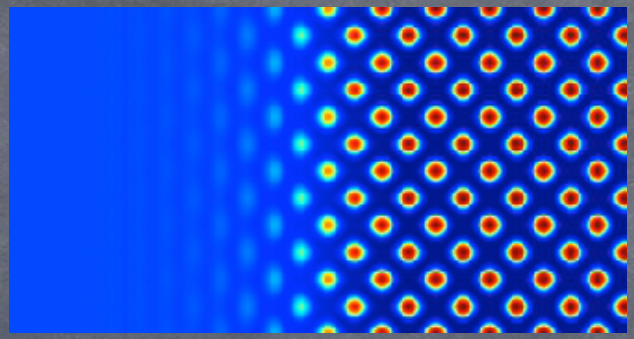

$$n(\mathbf{r}) = \bar{n} + \sum_j A(z)\exp(i\mathbf{K}_j \cdot \mathbf{r})$$

BCC Iron

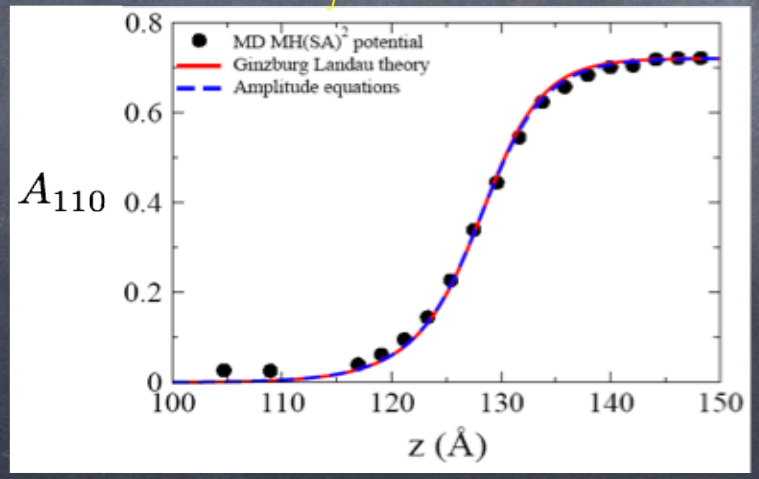

Wu and Karma, PRB 2007, MD simulations Asta

By expanding the structure function of Fe to eighth order, BCC crystal:

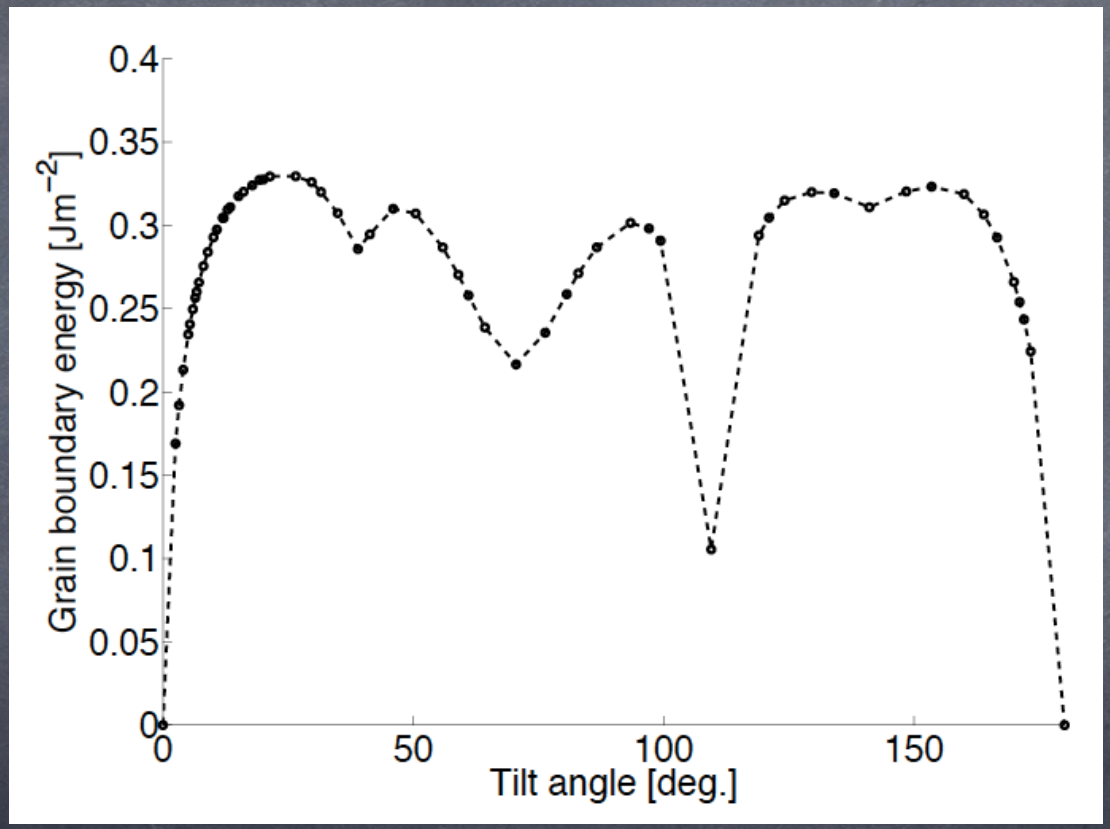

Results agree well with MD simulations using Finnis-Sinclair potential

A. Jaatinen C. V. Achim, K. R. Elder, T. Ala-Nissila

Beyond Swift-Hohenberg

Free energy density:

$$F(\mathbf{r}) = \frac{n^2(\mathbf{r})}{2} - \frac{\nu n^3(\mathbf{r})}{6} + \frac{\xi n^4(\mathbf{r})}{12} - \frac{n(\mathbf{r})}{2} \int_V C_2(|\mathbf{r} - \mathbf{r}'|) n(\mathbf{r}') d\mathbf{r}$$

Construct in Fourier space: $\hat{C}_2(k)$

$$\hat{C}_2(k) = \hat{C}_0 + \sum_{i=1}^{N} \exp\left(-\left(\frac{T}{T_{0i}}\right)^2\right) \exp\left(-\frac{(k-k_i)^2}{2{\alpha_i}^2}\right)$$

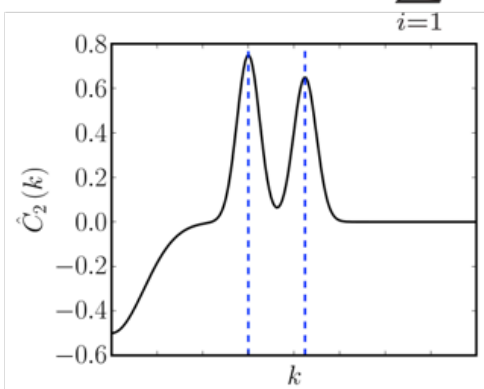

M. Greenwood, J. Rottler, and N. Provatas, *Phys. Rev. E* **83**, 031601 (2011)

K. Barkan, H. Diamant, R. Lifshitz, PRE (2011)

Generating Other Crystal Structures

Real space approach:

$$F = \int \left\{ \frac{n^2(\mathbf{r})}{2} \left[-\epsilon + (\nabla^2 + 1)^2 \right] n(\mathbf{r}) + \left[-\epsilon_n + (\nabla^2 + k_n)^2 \right]^n n(\mathbf{r}) + \frac{n^4(\mathbf{r})}{4} \right\}$$

Successfully generated:

- BCC
- FCC (n=1, Wu, Adland and Karma PRE 2010)
- Square lattice (Wu, Plapp and Voorhees, J. Phys. Cond Mat.)
- All Bravais lattices in 2D (n=2, Mkhonta, Elder and Huang, PRL 2013)

Complex Crystal Structures

$$F[n] = \int \left[\frac{1}{2}n^2 - \frac{1}{6}n^3 + \frac{1}{12}n^4\right] d\mathbf{r} - \frac{1}{2}\int n(\mathbf{r}) C_2 * n \; d\mathbf{r}$$

$$-\frac{1}{6}\iiint n(\mathbf{r}) C_3(\mathbf{r}-\mathbf{r}', \mathbf{r}-\mathbf{r}'') n(\mathbf{r}') n(\mathbf{r}'') d\mathbf{r} d\mathbf{r}' d\mathbf{r}''$$

M. Seymour and N. Provatas, PRB (2016)

Focus: stability angles between atoms to produce a better model of graphene

Approximate the three point correlation as

$$C_3(\mathbf{r}_1, \mathbf{r}_2) = \sum_i C_3^{(i)}(\mathbf{r}_1) C_3^{(i)}(\mathbf{r}_2)$$

Complex Crystal Structures

$$F[n] = \int \left[\frac{1}{2}n^2 - \frac{1}{6}n^3 + \frac{1}{12}n^4\right] d\mathbf{r} - \frac{1}{2}\int n(\mathbf{r}) C_2 * n \; d\mathbf{r}$$

$$-\frac{1}{6}\iiint n(\mathbf{r}) C_3(\mathbf{r}-\mathbf{r}', \mathbf{r}-\mathbf{r}'') n(\mathbf{r}') n(\mathbf{r}'') d\mathbf{r} d\mathbf{r}' d\mathbf{r}''$$

See Eli Alster's Poster

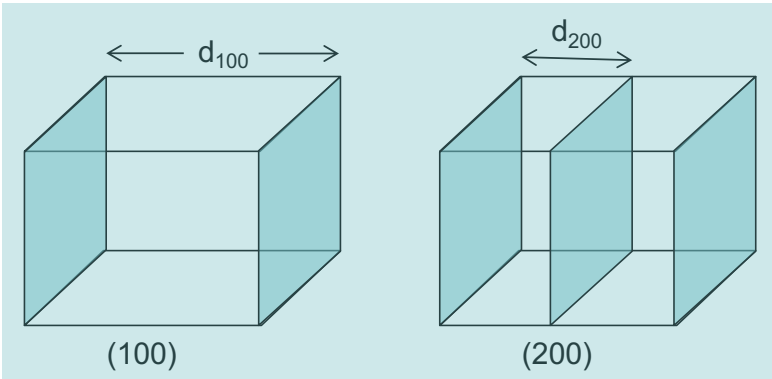

Two point: Interplanar length scales

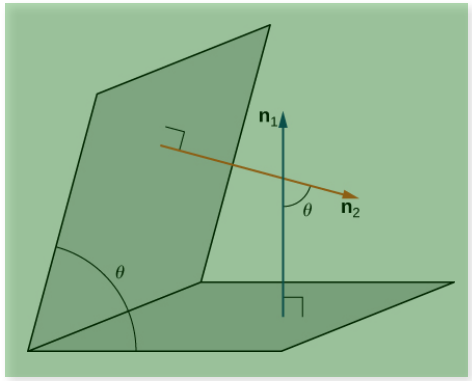

Three point: Interplanar angles

How to construct C_2, C_3?

Ex: Single component CaF_2, fcc with F in tetrahedral voids, Al_2Cu (θ')

- Look at structure factor

$$A_{(\mathfrak{h}\mathfrak{k}\mathfrak{l})} = \begin{cases} 12 & \text{if } \mathfrak{h}+\mathfrak{k}+\mathfrak{l} = 4N \\ & \text{and } \mathfrak{h},\ \mathfrak{k},\ \mathfrak{l} \text{ are all even} \\ 4 & \text{if } \mathfrak{h},\ \mathfrak{k},\ \mathfrak{l} \text{ are all odd} \\ -4 & \text{if } \mathfrak{h}+\mathfrak{k}+\mathfrak{l} = 4N+2 \\ & \text{and } \mathfrak{h},\ \mathfrak{k},\ \mathfrak{l} \text{ are all even} \\ 0 & \text{otherwise.} \end{cases}$$

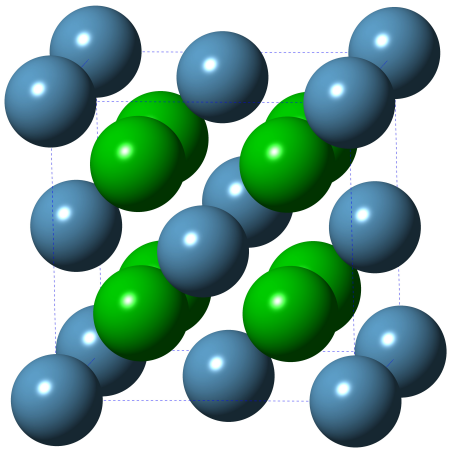

- **Conventionally:** When $A_{(hkl)} \neq 0$, make a peak at **q**(hkl) in C_2. In CaF_2, {111}, {200}, …

Choosing C_2

Problem: {111}, {200}, are the same wavevectors as for fcc!

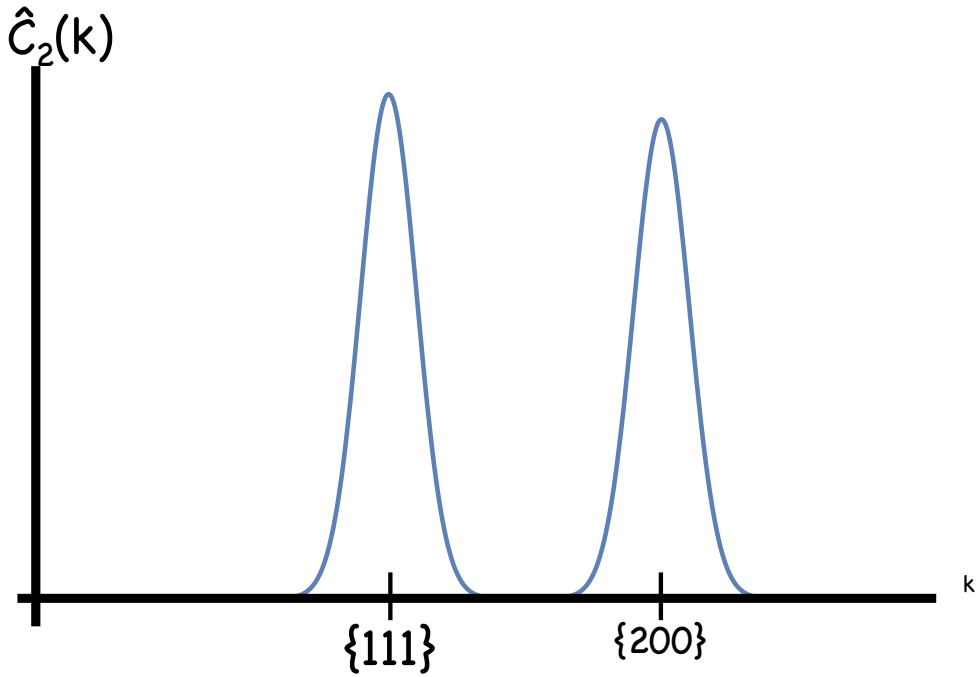

How to get CaF_2?

Choosing C_3

- Use FCC $\hat{C}_2$, distinguish between structures with C_3
- Convenient to construct C_3 in Fourier space

$$\hat{C}_3(\mathbf{k}_p, \mathbf{k}_q) = R(k_p)R(k_q)\sum_{l=0}^{l_{\max}} \alpha_l P_l(\hat{\mathbf{k}}_p \cdot \hat{\mathbf{k}}_q)$$

$$F_3/V = -\frac{1}{6}\sum_{pqr} \hat{C}_3(k_p, k_q, \hat{\mathbf{k}}_p \cdot \hat{\mathbf{k}}_q) A_p A_q A_r \delta_{\mathbf{k}_p+\mathbf{k}_q+\mathbf{k}_r,\mathbf{0}}$$

- **Aim:** Design $\hat{C}_3$ such $F_3(CaF_2) < F_3(FCC)$
- **How:** They differ in their three-point structure
  - FCC: $A_{(111)}A_{(1\bar{1}\bar{1})}A_{(\bar{2}00)} > 0$
  - CaF_2: $A_{(111)}A_{(1\bar{1}\bar{1})}A_{(\bar{2}00)} < 0$

Choosing C_3

$$\hat{C}_3(\mathbf{k}_p, \mathbf{k}_q) = R(k_p)R(k_q)\sum_{l=0}^{l_{\max}} \alpha_l P_l(\hat{\mathbf{k}}_p \cdot \hat{\mathbf{k}}_q)$$

complete

$$F_3/V = -\frac{1}{6}\sum_{pqr} \hat{C}_3(k_p, k_q, \hat{\mathbf{k}}_p \cdot \hat{\mathbf{k}}_q) A_p A_q A_r \delta_{\mathbf{k}_p+\mathbf{k}_q+\mathbf{k}_r,\mathbf{0}}$$

Choose α_l so that there is a negative peak at $\hat{\mathbf{k}}_p \cdot \hat{\mathbf{k}}_q = (111) \cdot (1\bar{1}\bar{1}) = -1/3$

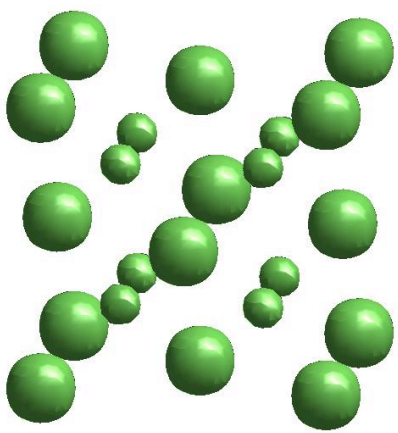

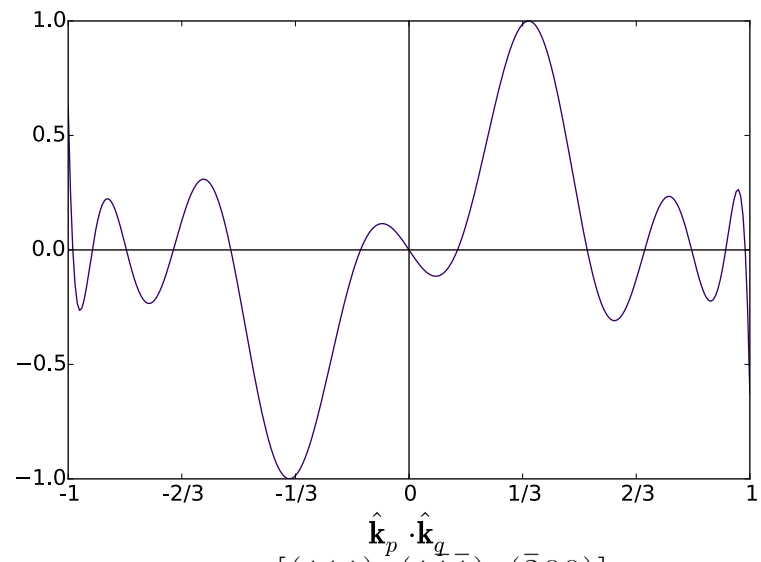

$[(111), (1\bar{1}\bar{1}), (\bar{2}00)]$

Crystal Structures

- Disordered CaF_2, simple cubic, diamond cubic, graphene layers
- Perovskite:

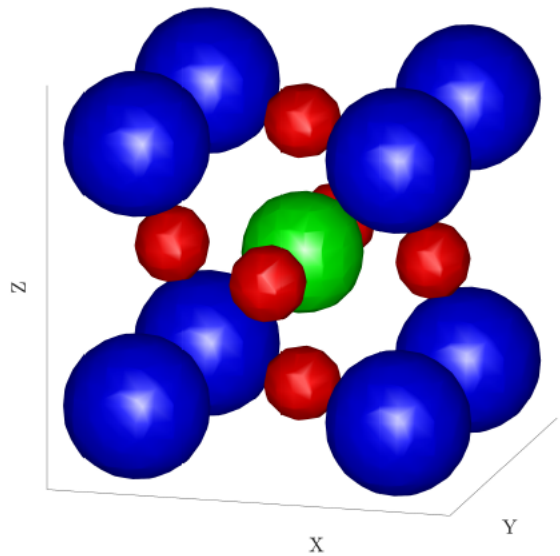

PFC: Ordered Crystal Structures

First Order

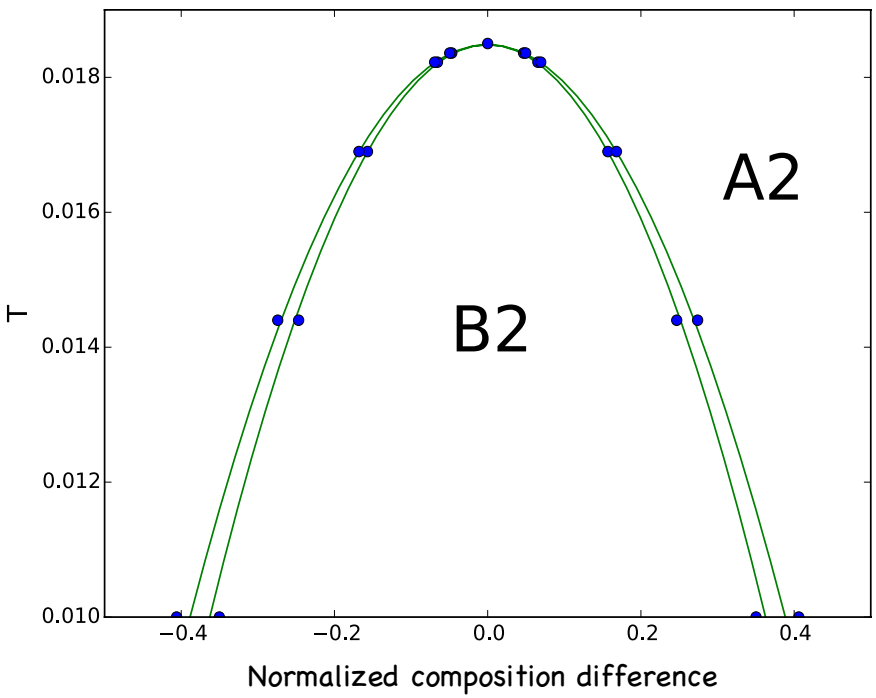

Second Order

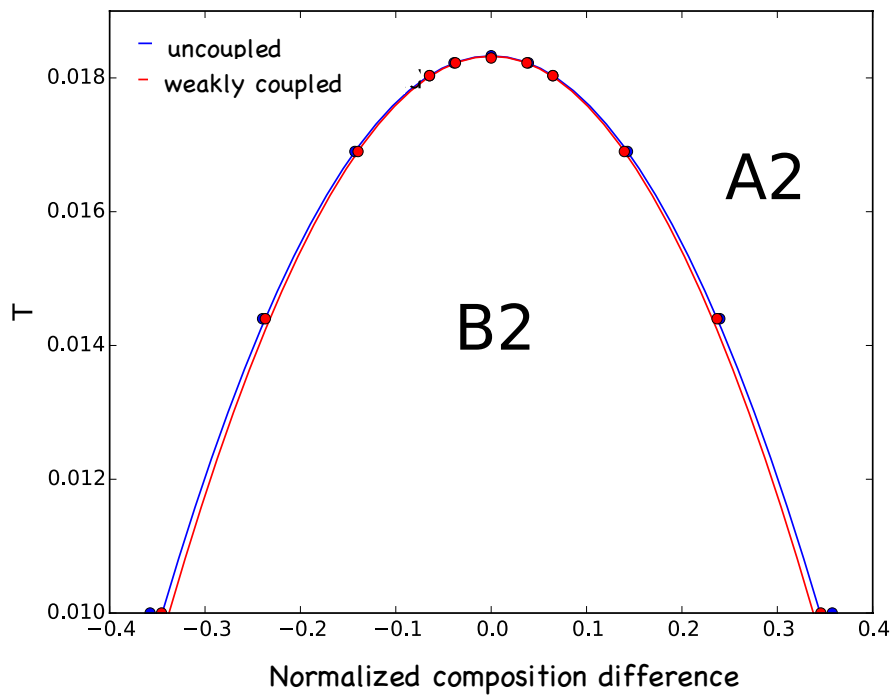

Alster, Eli, et al. *Physical Review E* 95.2 (2017): 022105.

The PFC and Classical Potentials

- Classical potentials are created by fitting to known materials parameters
- This can be a challenging task, e.g. Si: simulations of bulk Si employ Stillinger-Weber potentials, but simulations of Si-vacuum surfaces employ Tersoff potentials
- The problem is similar in the PFC where free energy functions need to be chosen to yield a given set of properties or crystal structures

Dynamics

Free energy functional:

$$F = \int \left\{ \frac{n(\mathbf{r})}{2} \left[-\epsilon + \left(\nabla^2 + 1\right)^2 \right] n(\mathbf{r}) + \frac{1}{4} n^4(\mathbf{r}) \right\} d\mathbf{r}$$

Free energy decrease, completely diffusive dynamics:

$$\frac{\partial n}{\partial t} = \nabla \cdot \nabla \frac{\delta F}{\delta n} = \nabla \cdot \nabla \left\{ \left[-\epsilon + (\nabla^2 + 1)^2 \right] n + n^3 \right\}$$

Free energy decrease, two time scales: elasticity and diffusion,

$$\beta \frac{\partial^2 n}{\partial t^2} + \alpha \frac{\partial n}{\partial t} = \nabla \cdot \nabla \{ [-\epsilon + (\nabla^2 + 1)^2] n + n^3 \}$$

Stefanovic, Haataja and Provatas, PRL, 2006

Energy of low angle grain boundaries

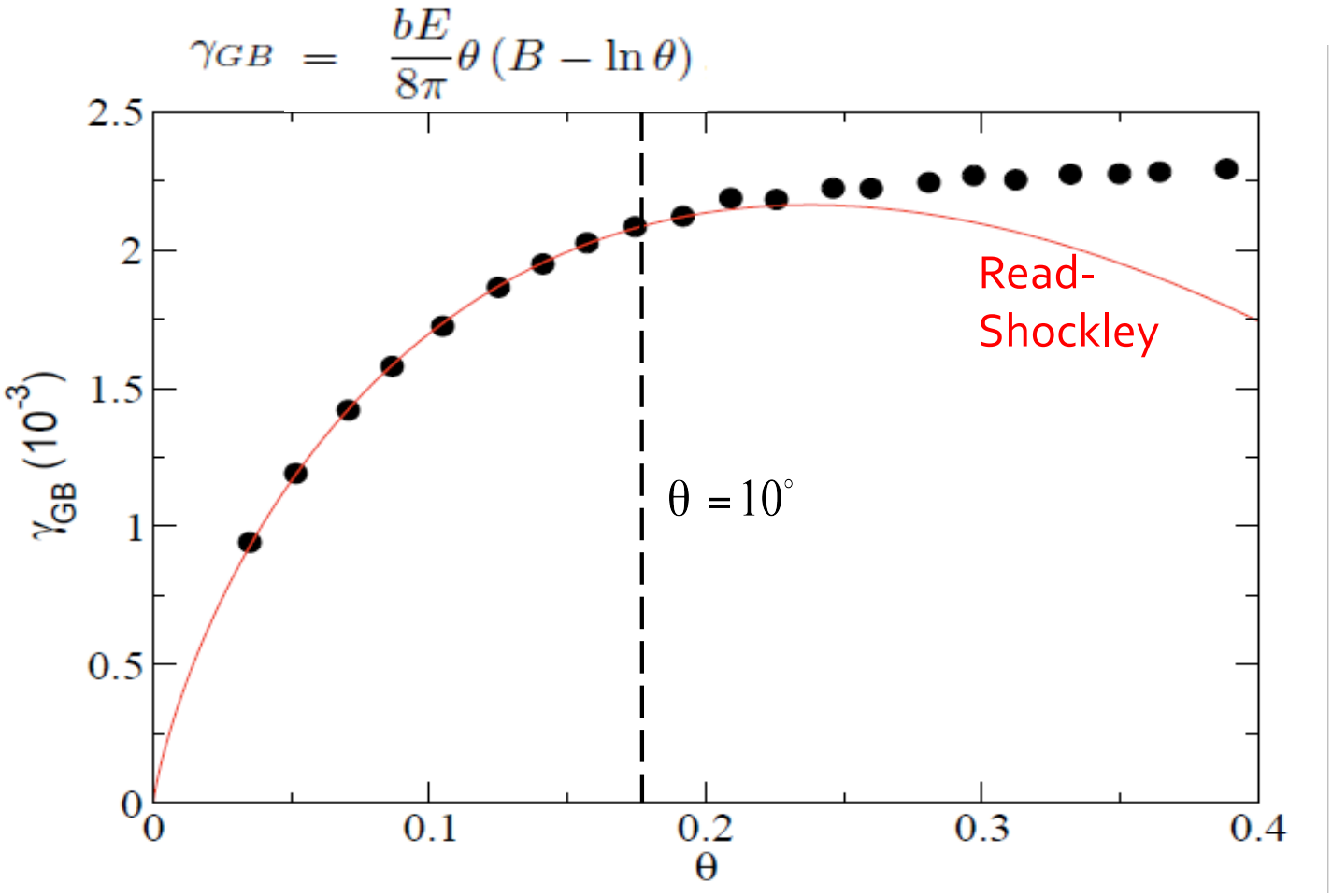

Coupling between grain boundary motion and grain rotation

Continuity of the lattice across the grain boundary results in a coupling of the normal motion of a grain boundary with the tangential motion of the lattice.

$$v_t = \beta v_n$$

$$\beta = 2\tan\left(\theta/2\right) \approx \theta$$

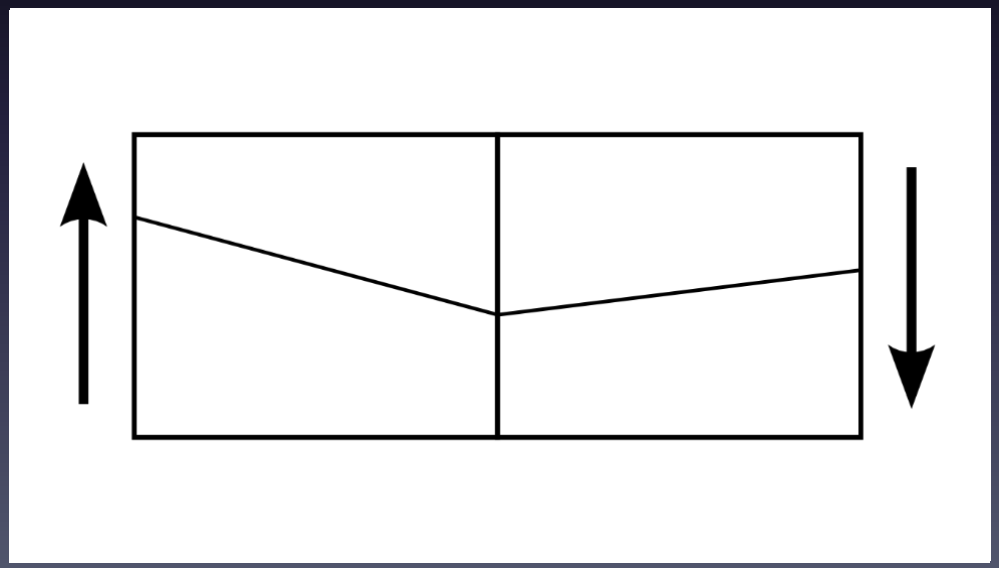

Single Grain

$$\theta = b / d$$

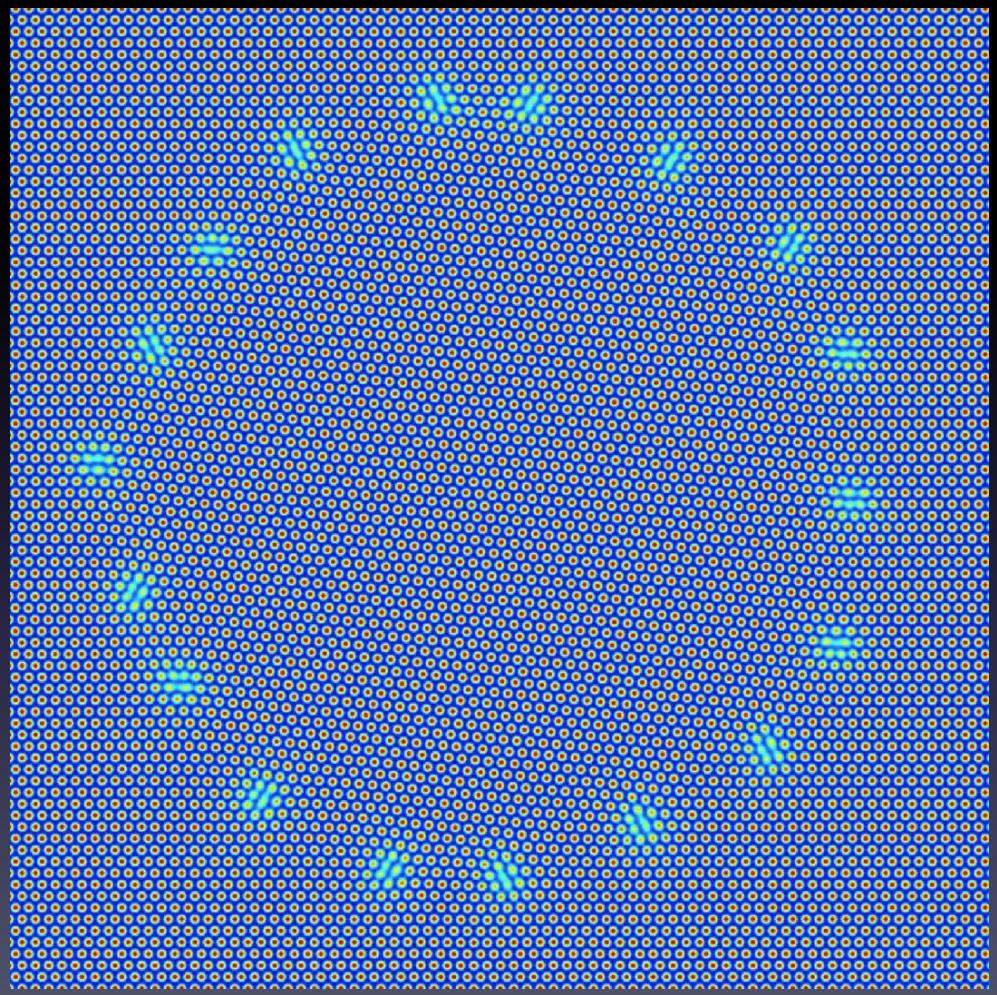

Wu KA, Voorhees PW. Acta Materialia. 2012;**60**:407-19.

Lattice Coupling Induced Rotation

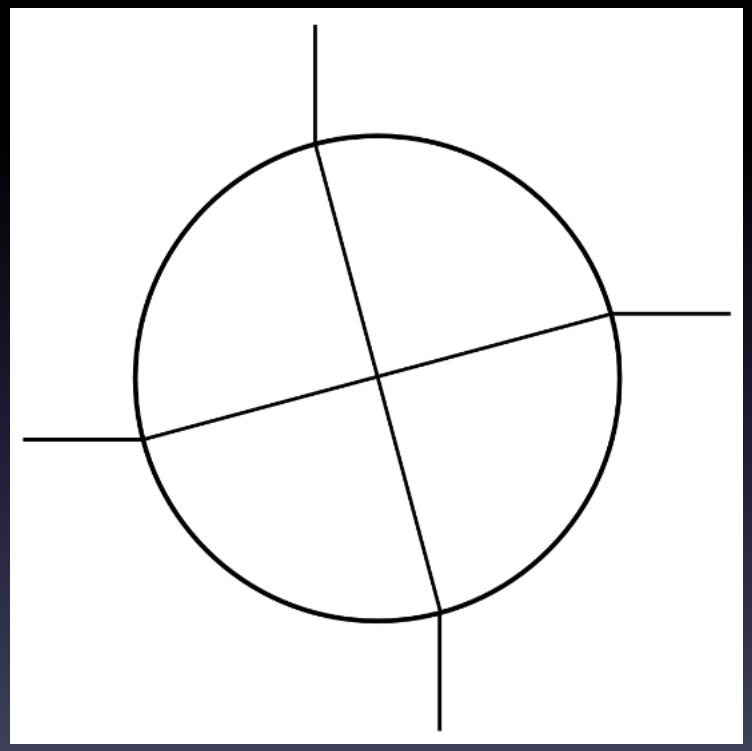

J. Cahn and J. Taylor, *Acta Mater.* **52**, 4887 (2004)

$1 - \epsilon - 0.87$

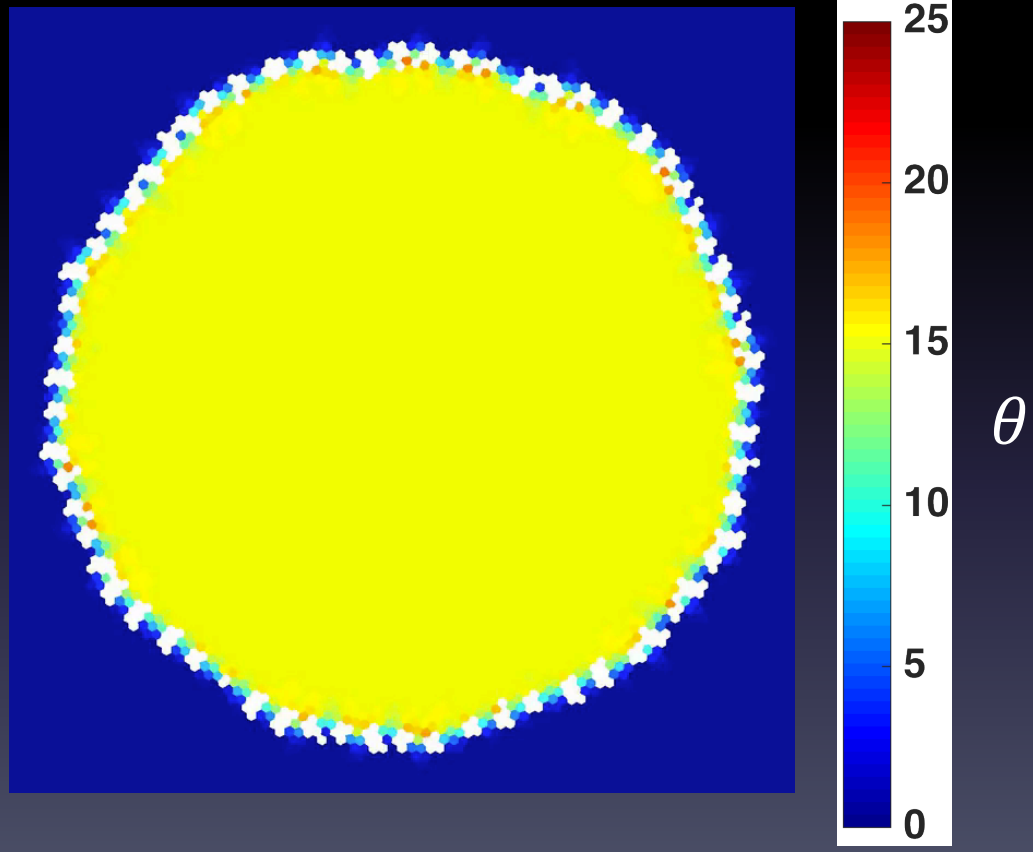

Molecular Dynamics Simulations

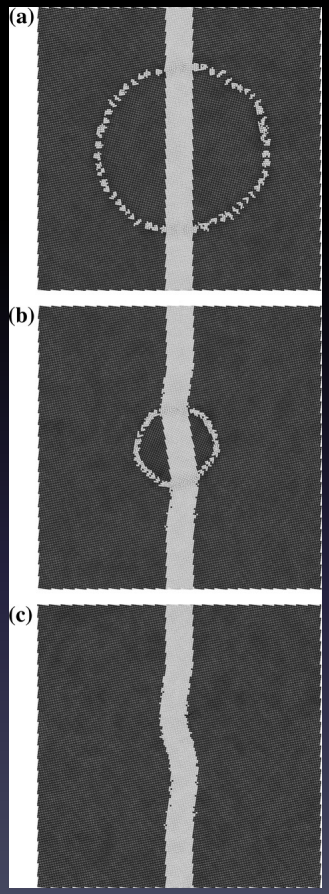

Z.T. Trautt and Y. Mishin, Acat Mater. **60** 2407 (2012)

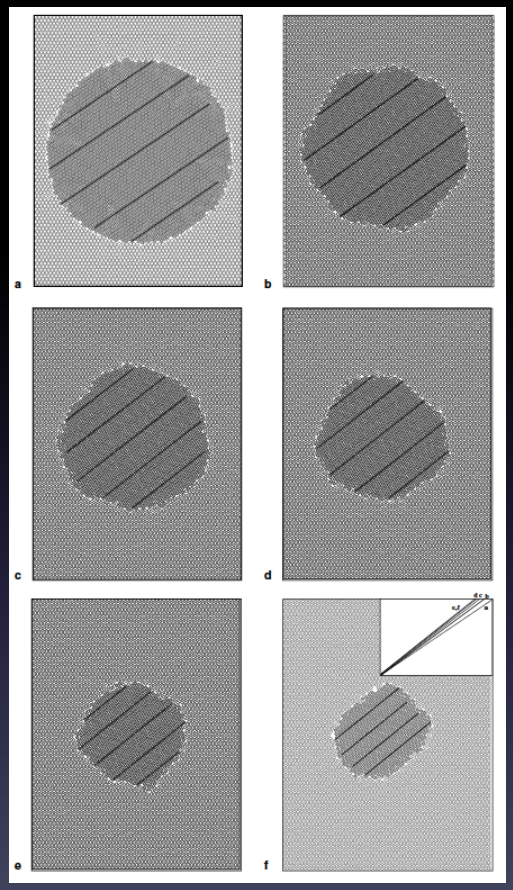

M. Upmanyu, D.J. Srolovitz, A.E. Lobkovsky, J.A. Warren, W.C. Carter, Acta Mater. **54** 1707 (2006)

3D Structure of Low Angle Planar Boundaries in BCC Crystals

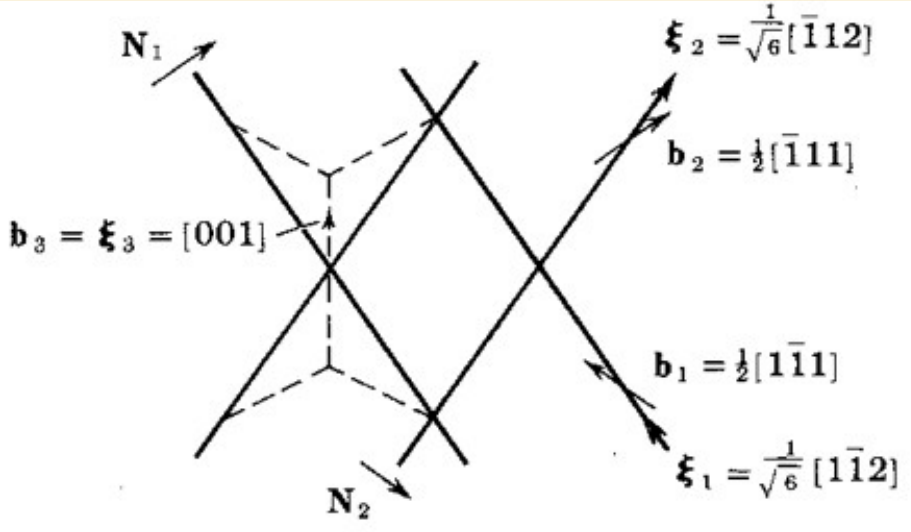

Fig. 19-25. Twist boundary on a (110) plane in a bcc crystal, showing a reaction in a lozenge-shaped net to form the dislocations $\mathbf{b}_3 = [001]$.

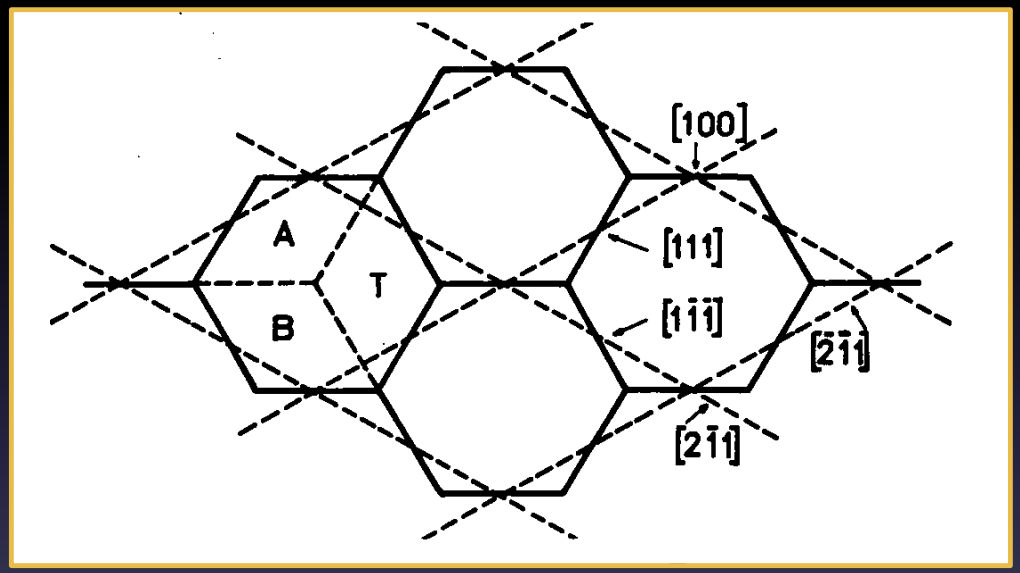

J. P. Hirsh and J. Lothe, Theory of dislocations, McGraw-Hill, (1968), p. 663.

S. Amelinckx and W. Dekeyser, Solid State Physics, 8 (1959), p. 349.

BCC Iron

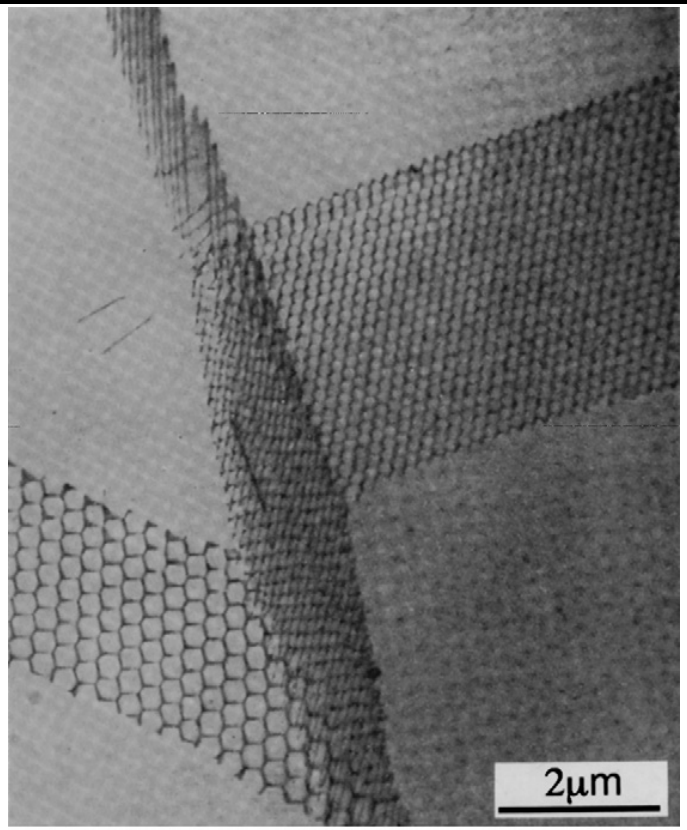

Figure 9.9 Transmission electron micrograph of extensive dislocation networks in body-centred cubic iron. Each network consists of three sets of dislocations, Burgers vectors $\frac{1}{2}\langle 111\rangle, \frac{1}{2}\langle 1\bar{1}\bar{1}\rangle$ and $\langle 100\rangle$. The plane of the networks is almost parallel to the plane of the foil. (Courtesy Dadian and Talbot-Besnard.)

D. Hull and D. J. Bacon, Introduction to Dislocations, Butterworth-Heinemann, Oxford, 2001, p. 167.

5° misorientation

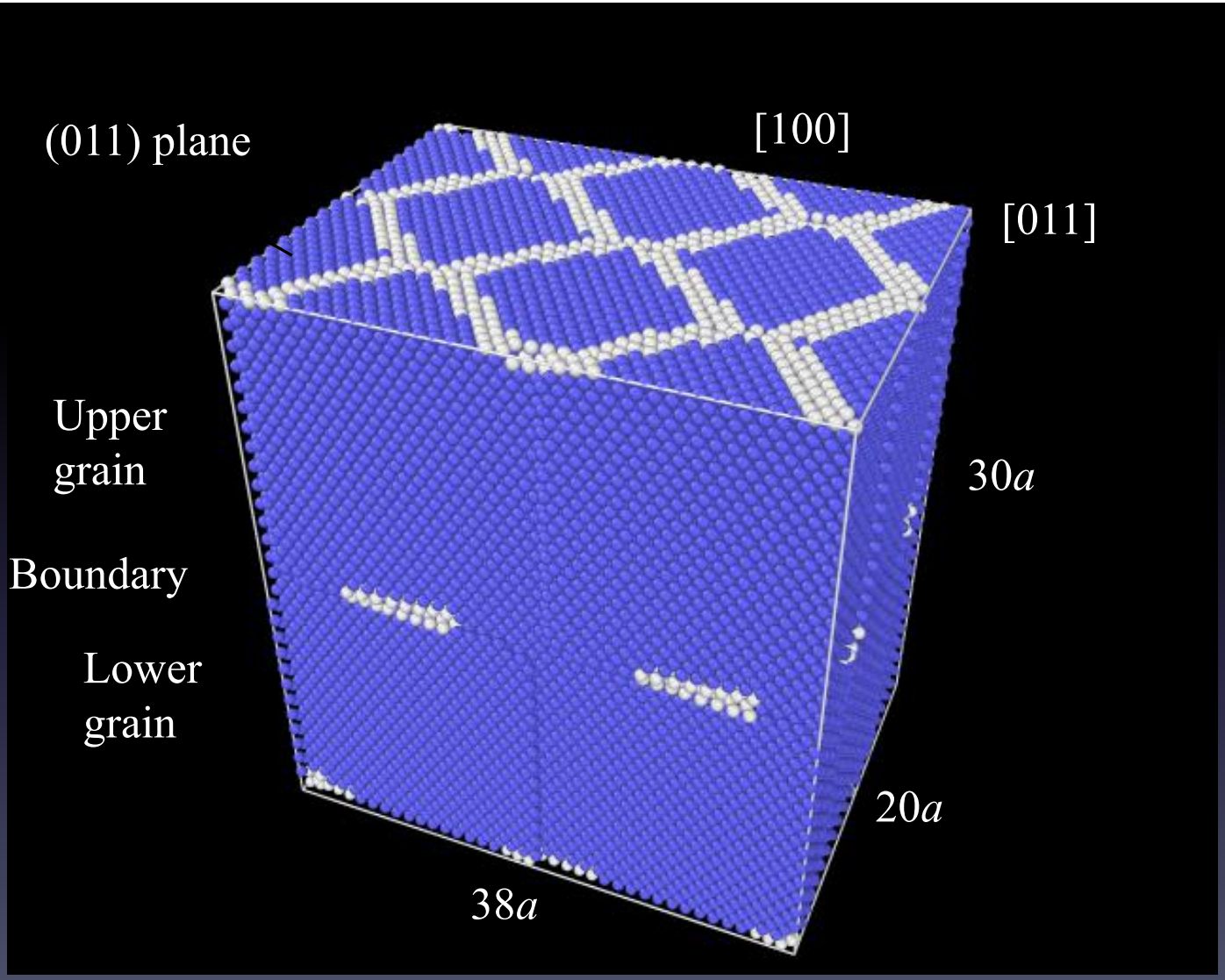

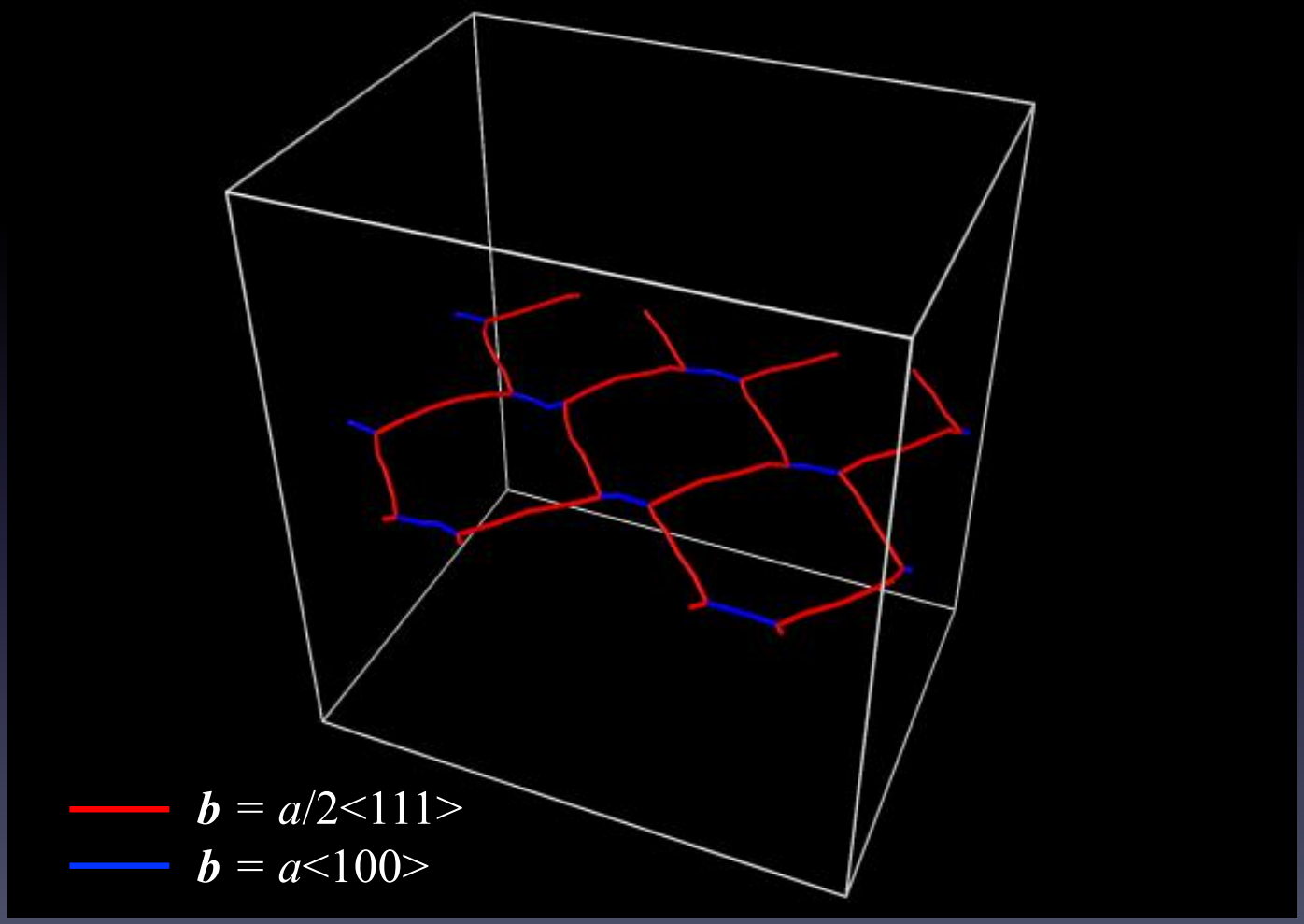
b = *a*/2<111>
b = *a*<100>

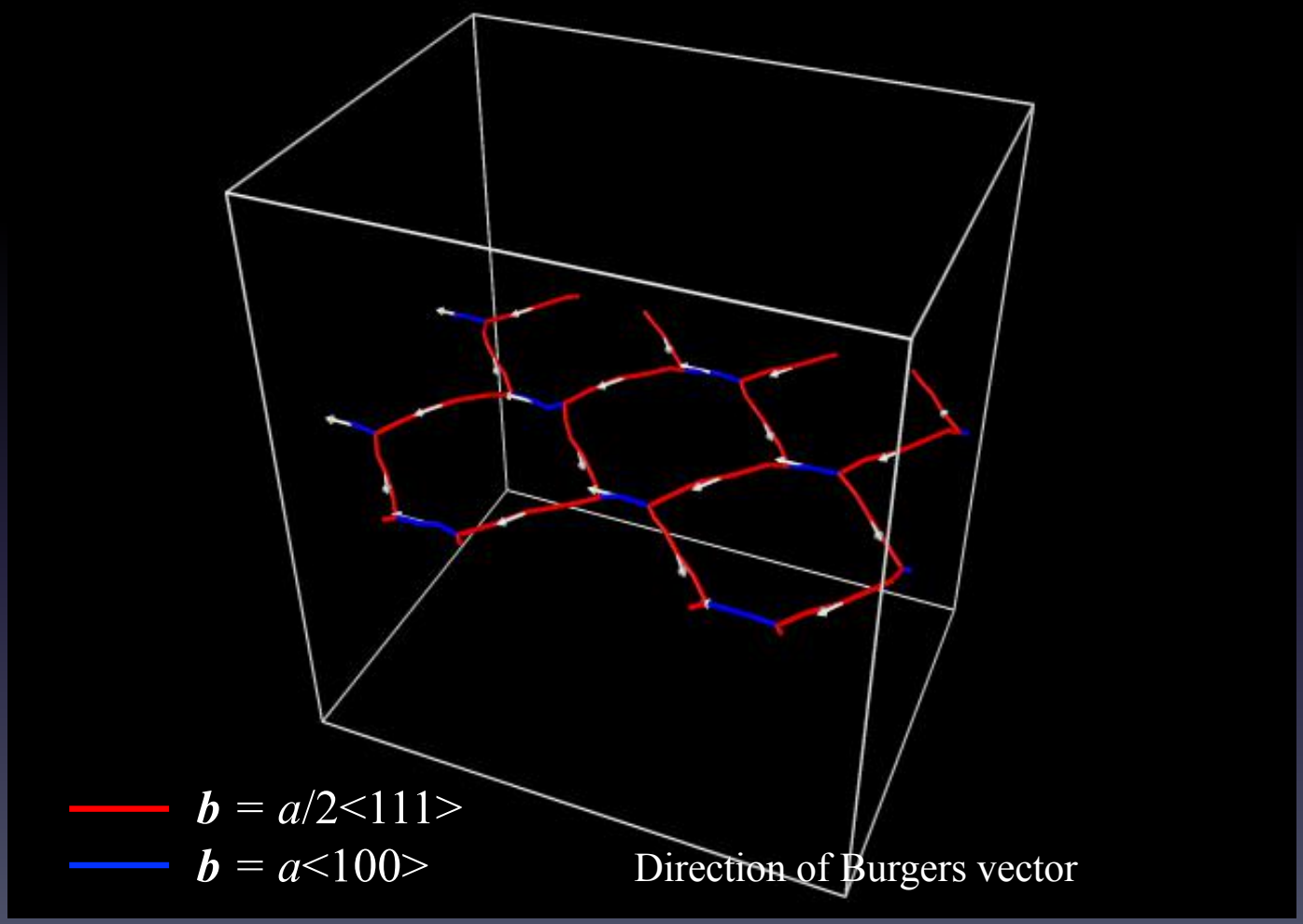
$\boldsymbol{b} = a/2\langle 111\rangle$
$\boldsymbol{b} = a\langle 100\rangle$
Direction of Burgers vector

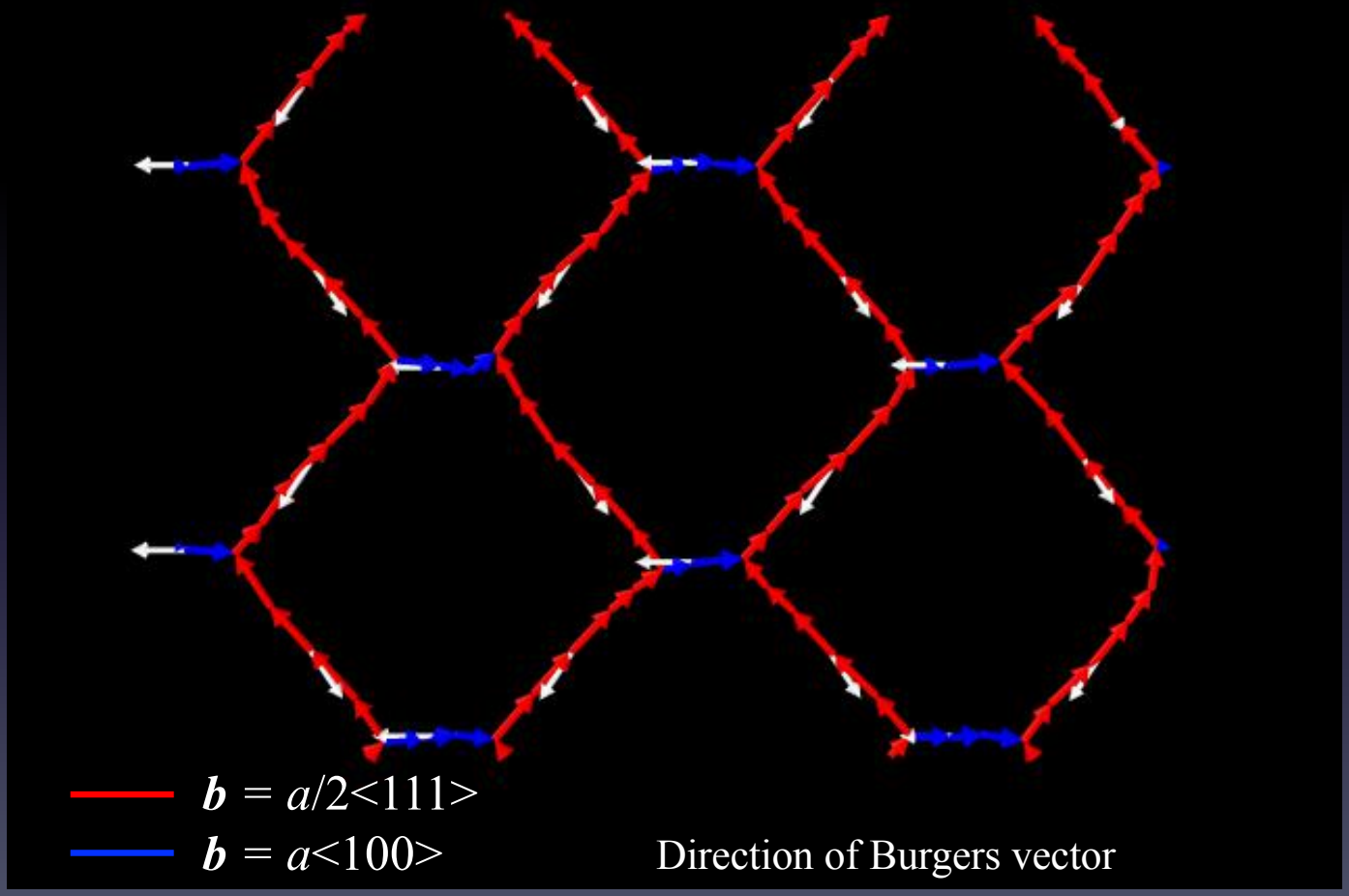
$\boldsymbol{b} = a/2\langle 111\rangle$
$\boldsymbol{b} = a\langle 100\rangle$
Direction of Burgers vector

10° Rotation about [110]

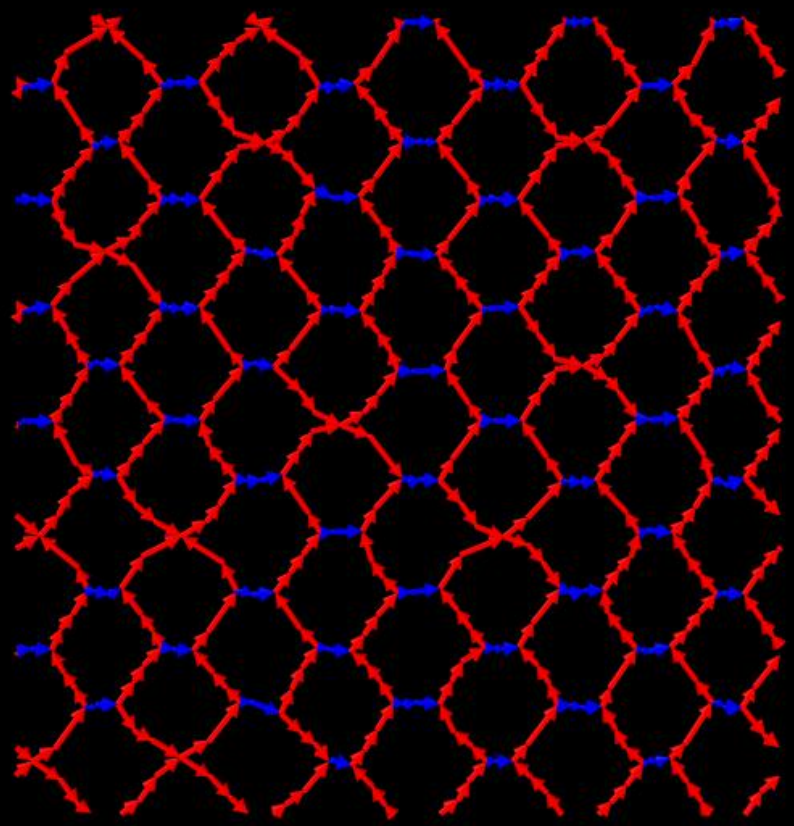

Initially Spherical Grain Embedded in Another

- Rotate about [110]
- Lattice constant BCC Fe
- 627^3 grid using a GPU

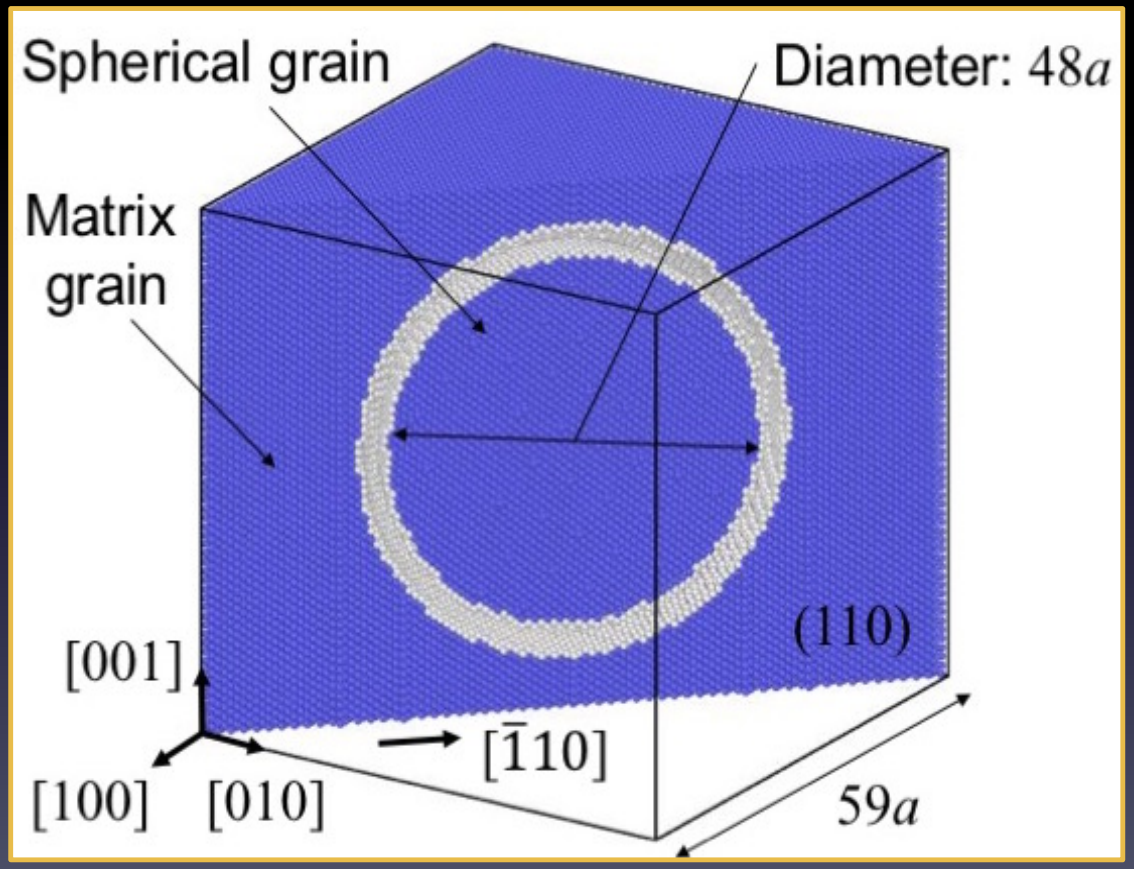

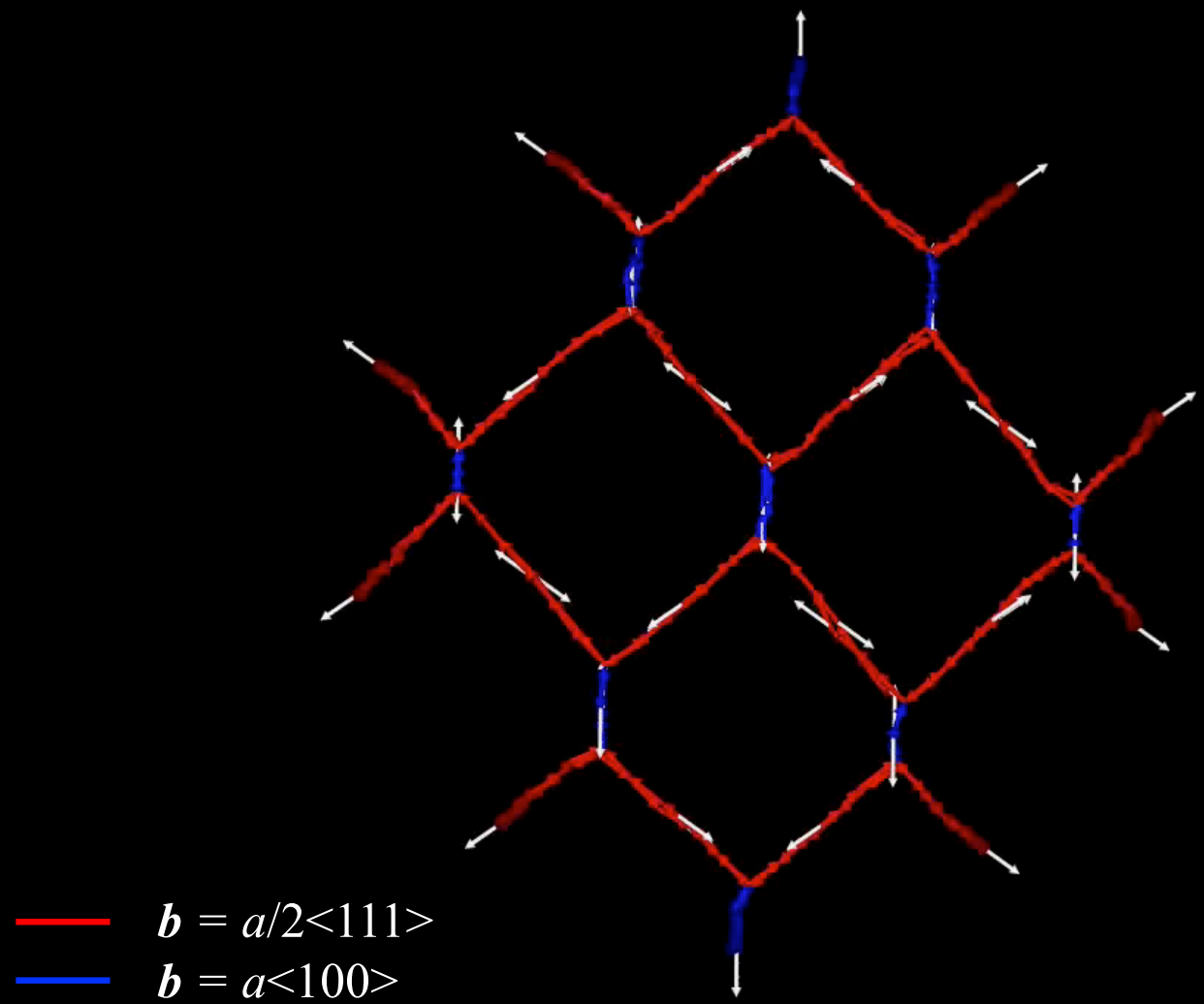

b = $a/2\langle 111\rangle$

b = $a\langle 100\rangle$

4º Rotation about [110]

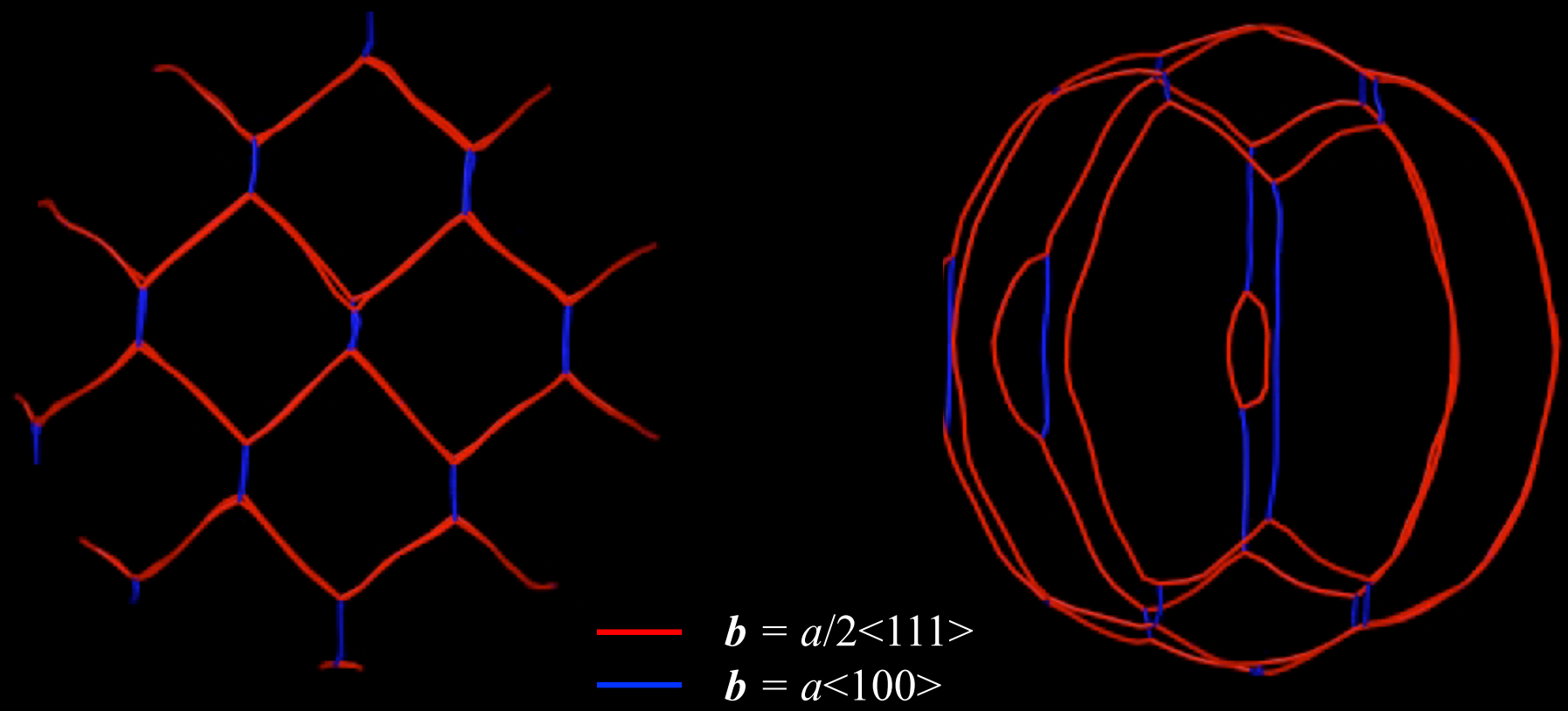

4º Rotation about [110]

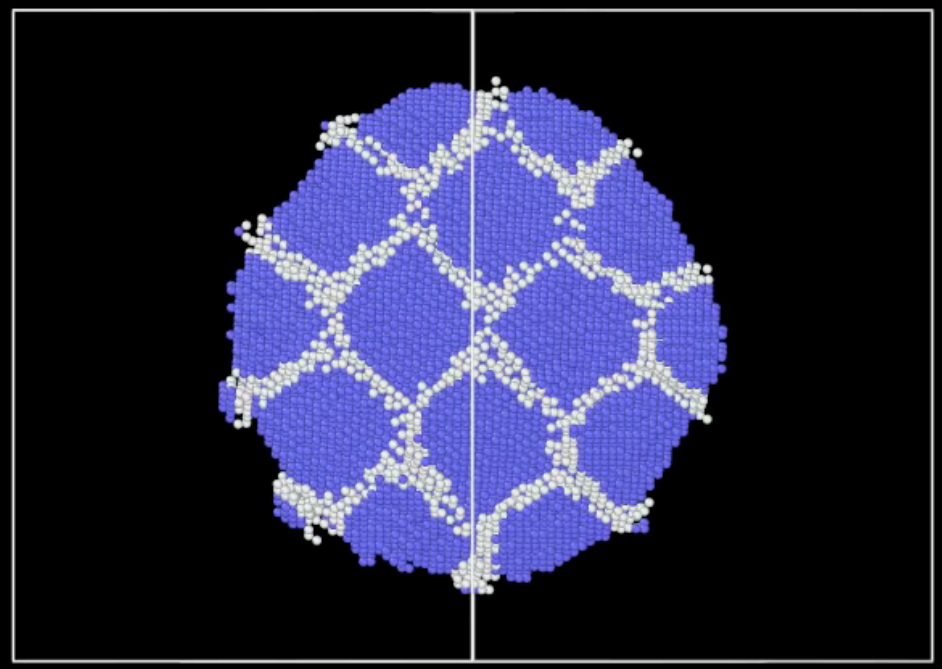

Seen from above, along [110]

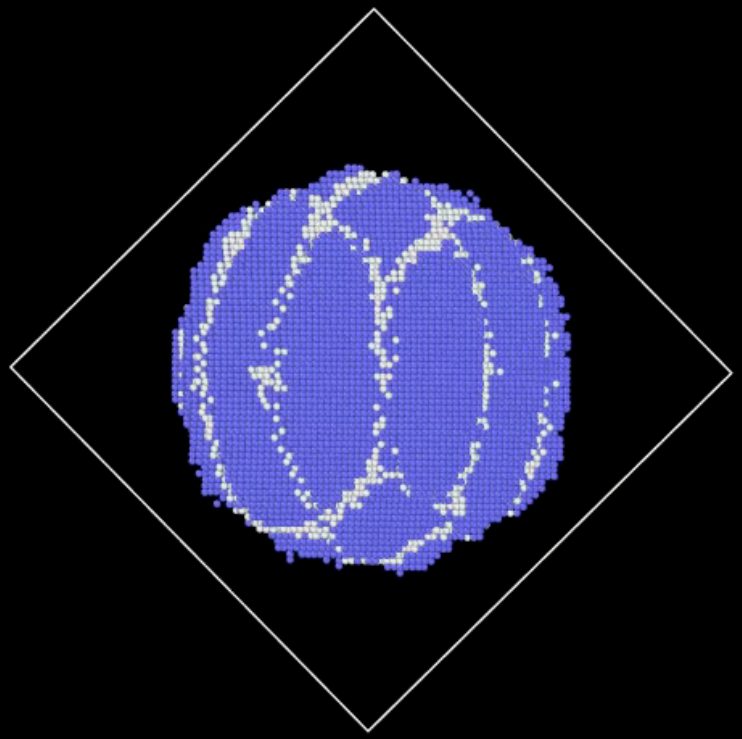

Seen from side, along [100]

Dislocation reactions

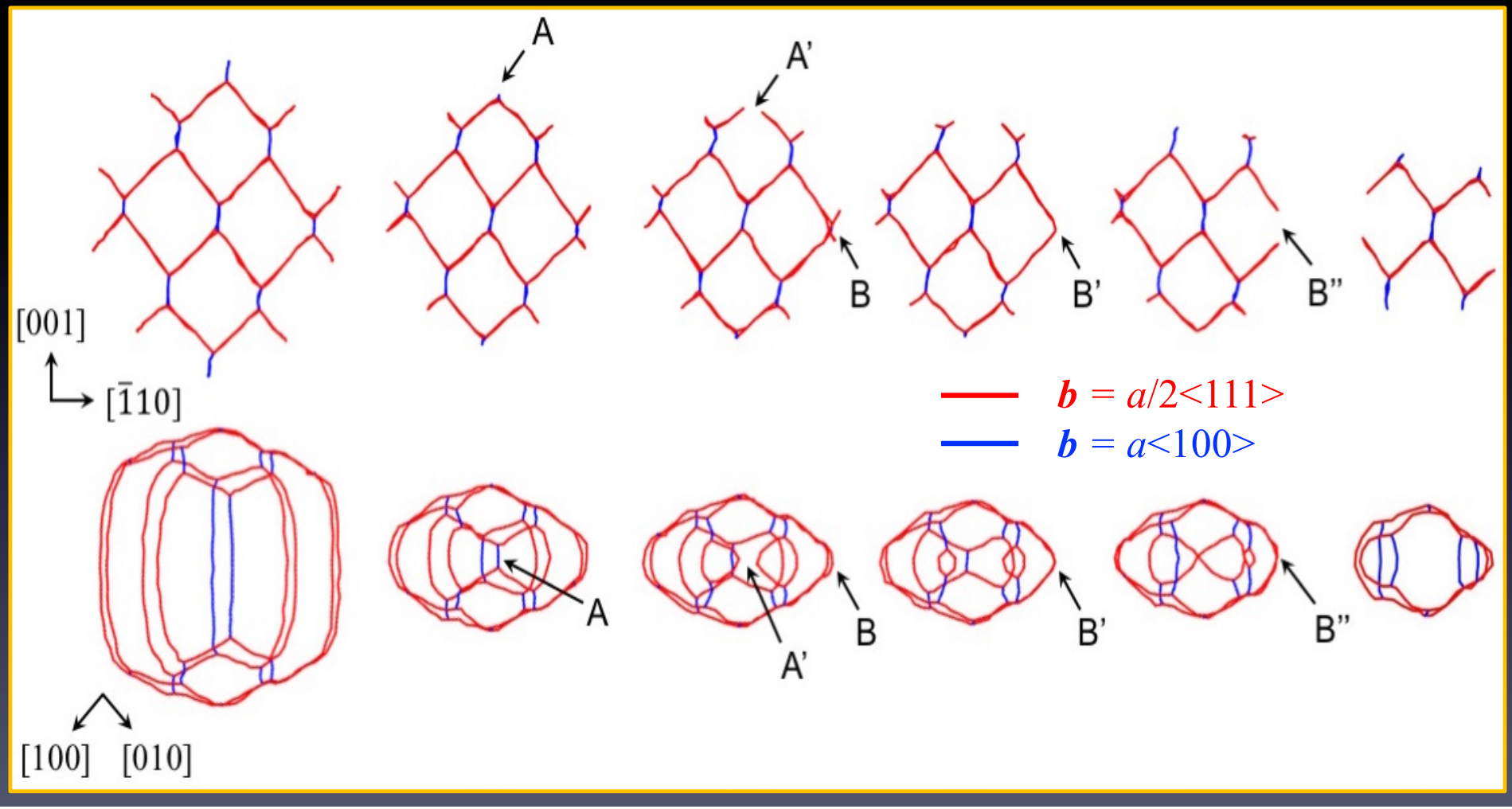

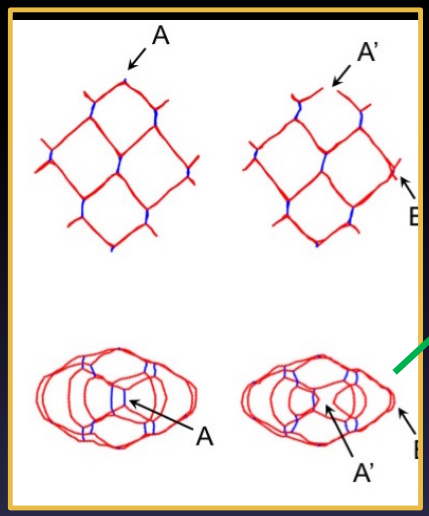
A
A'
A
A'

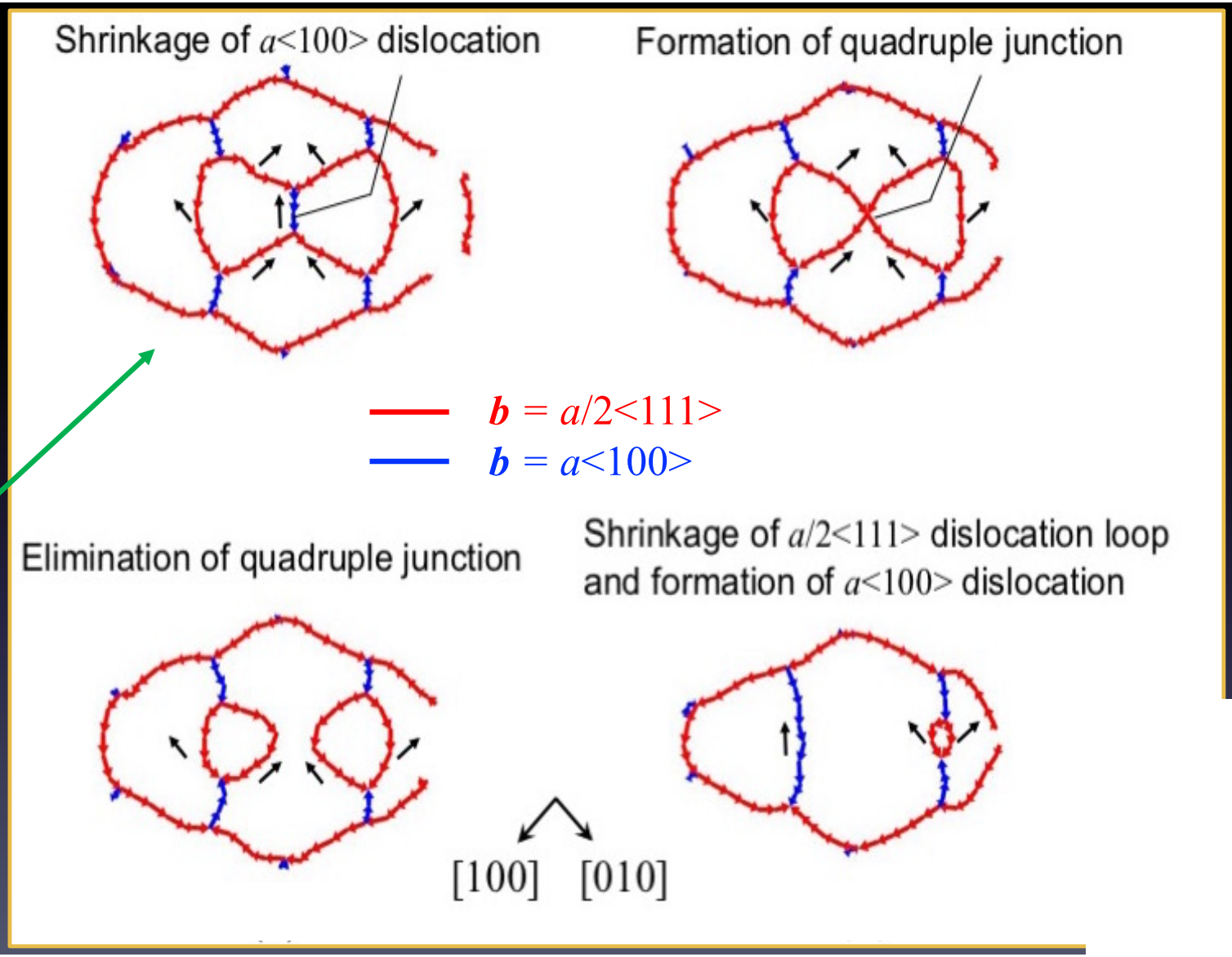
Shrinkage of a<100> dislocation
Formation of quadruple junction
b = a/2<111>
b = a<100>
Elimination of quadruple junction
Shrinkage of a/2<111> dislocation loop
and formation of a<100> dislocation
[100]
[010]

10º Rotation about [110]

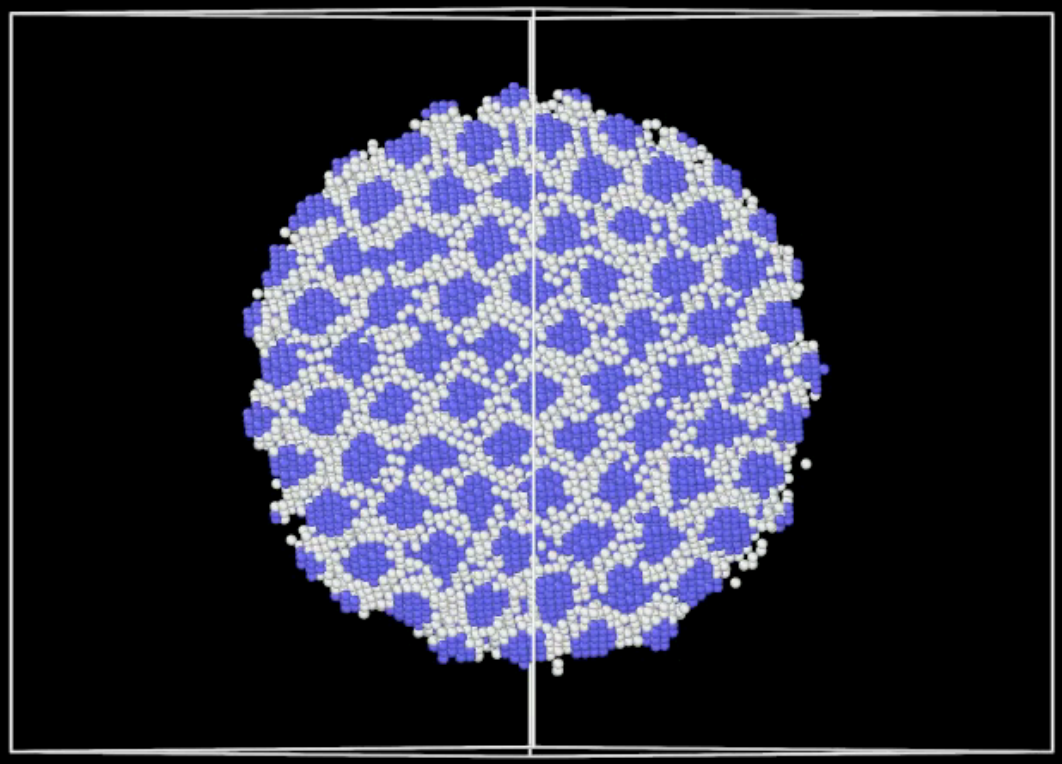

Seen from above, along [110]

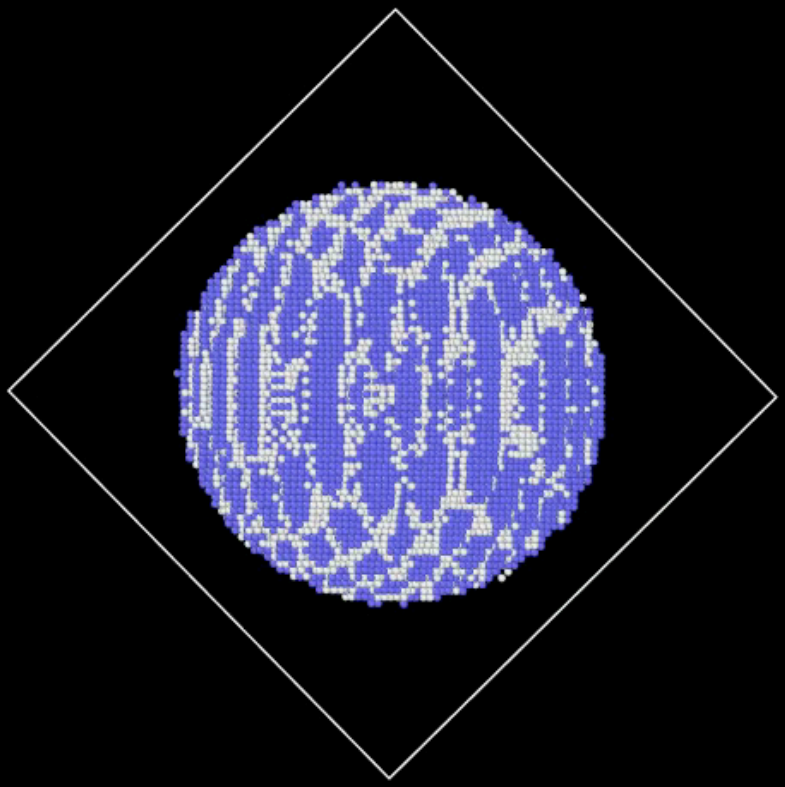

Seen from side, along [100]

Dynamics: Surface area and Grain Rotation

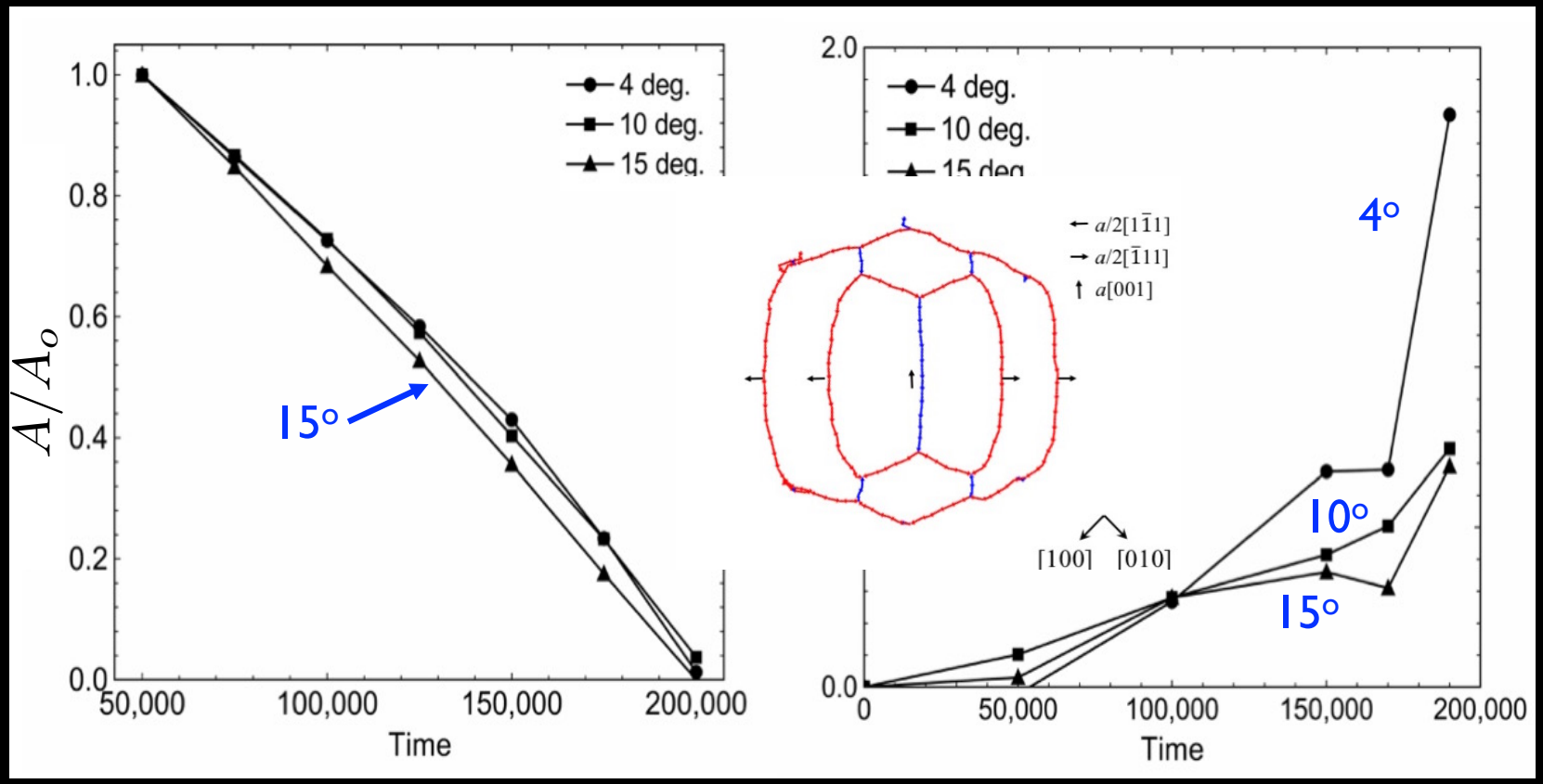

Classical result: $A(t) = A(0) - kt$

Effects of Decreasing Temperature: 4º Rotation about [110]

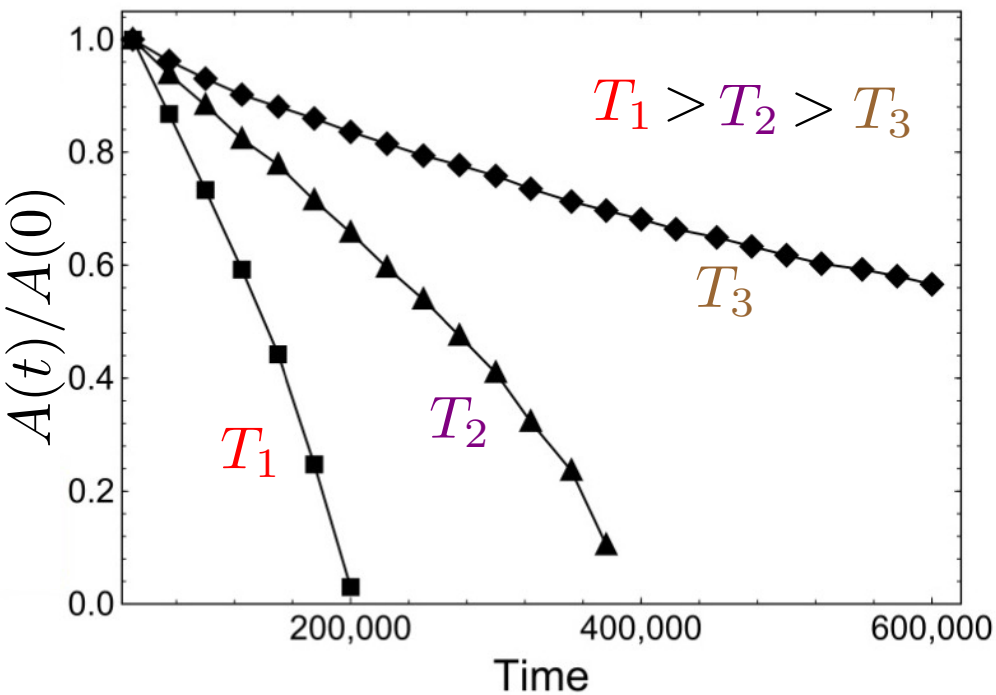

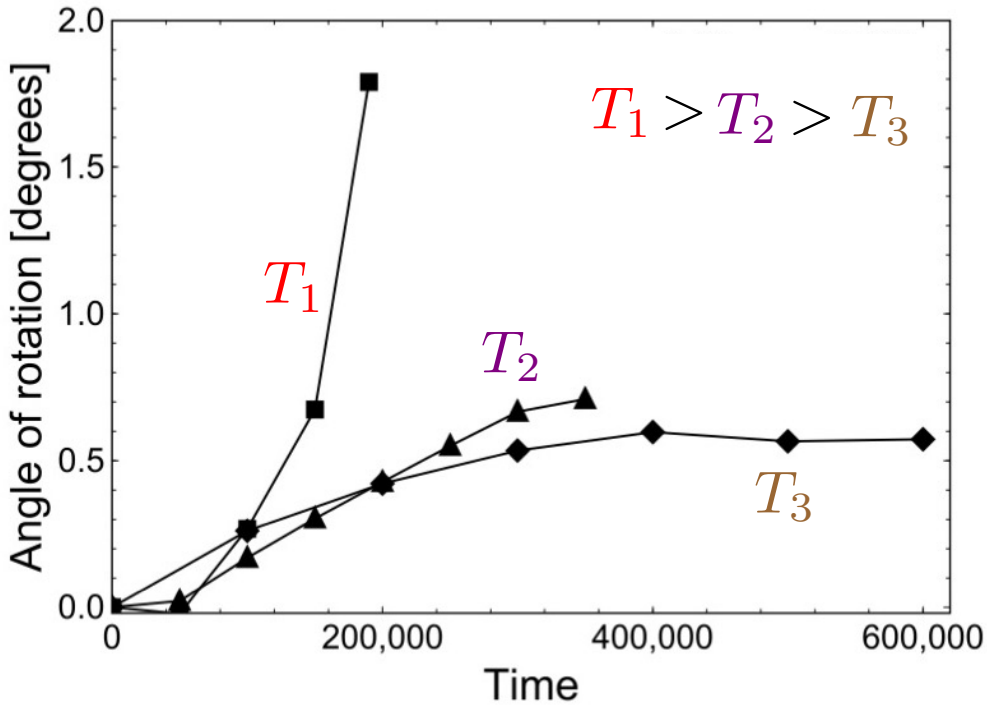

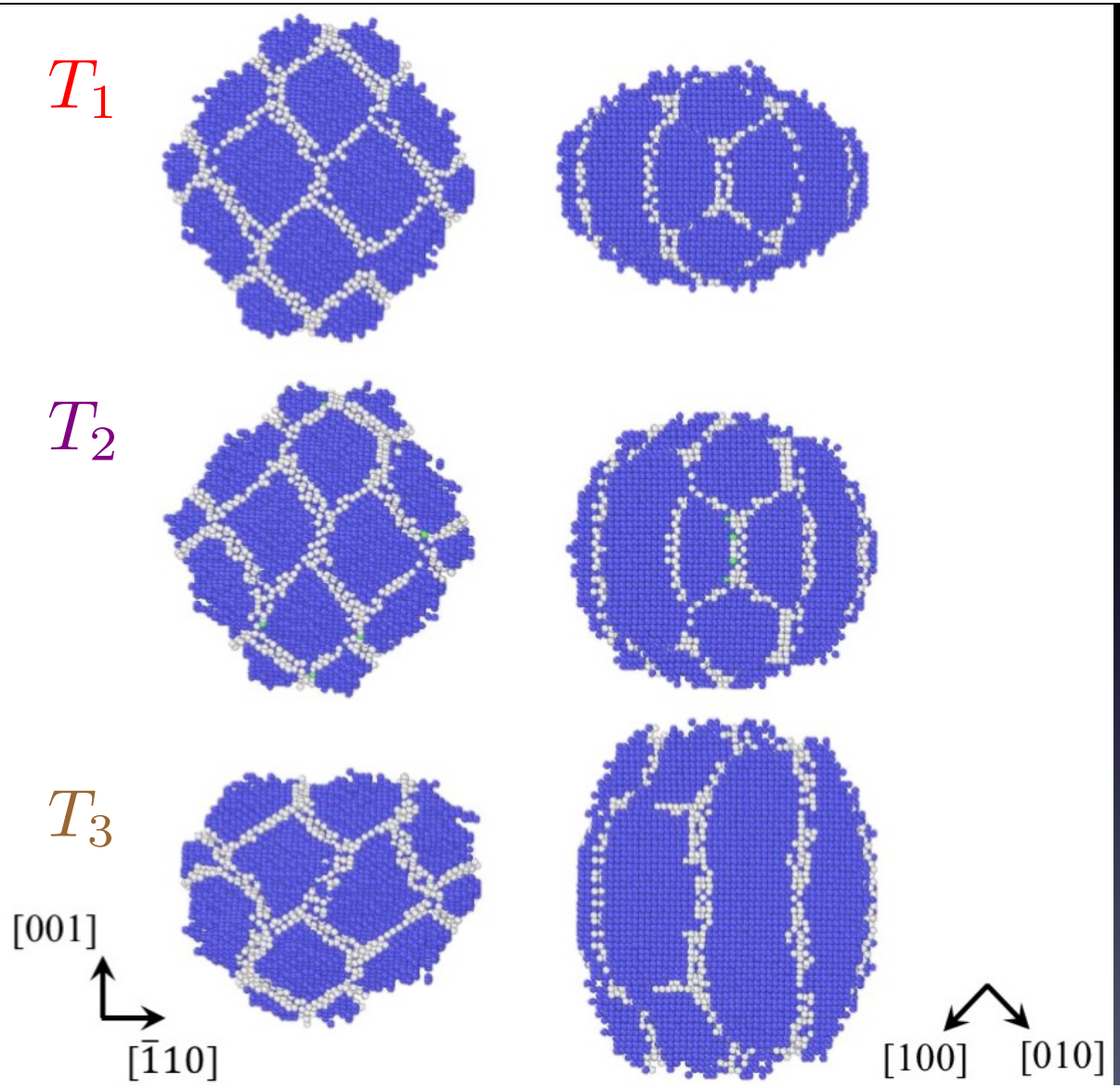
T_1
T_2
T_3
[001]
[$\bar{1}$10]
[100]
[010]

Conclusions

- Phase field crystal method can extended to account for complex crystal structures
- Grain rotation during grain growth
- Grain translation during grain growth
- Dislocation climb is essential for grain shrinkage in this case
- Lower temperature simulations show the effects of dislocation interactions on grain growth

Challenges

- Vacancies: Fixing a realistic vacancy concentration
- Dynamics: Modeling solidification in a pure material; Separating the climb and glide of dislocations
- Fluctuations
- A method for choosing the potentials to model a specific material (see graphene)
- Defects: Is the core structure of dislocations realistic? Is dislocation nucleation realistic?